PHASED-LOCKED LOOP STUDY, SIMULATION, AND DESIGN OF ADAPTIVE FILTER

by

Thomas Wayne Arthur

Thesis submitted to the Graduate Faculty of the
Virginia Polytechnic Institute
in Candidacy for the Degree of

MASTER OF SCIENCE

in

Electrical Engineering

APPROVED:

Dr. W. W. Cannon, Chairman

Dr. H. K. Ebert

Prof. Ralph R. Wright

Dr. Herbert Krauss

February 1967

Blacksburg, Virginia

TABLE OF CONTENTS

LIST OF FIGURES

Page

LIST OF TABLES

LIST OF SYMBOLS

A	Gain of d-c amplifier
B_i	Bandwidth of filter preceding phase-locked loop, hertz
B_L	Loop noise bandwidth, hertz
f	Frequency, hertz
$F(s)$	Transfer function of loop filter
$H(s)$	Phase transfer function of loop
K_{pd}	Phase detector gain factor, volts/radian
K_{vco}	Voltage controlled oscillator gain factor rad/sec./volt
K_v	D-c loop gain, $sec.^{-1}$
$\eta(t)$	Noise voltage
P_s	Signal power, watts
P_n	Noise power, watts
PLL	Phase-locked loop
s	Laplace complex variable
SNR_i	SNR at input) SNR - signal-to-noise ratio
$(SNR)_L$	SNR in loop)
t_p	Pull-in time, sec.
v_2	Input to VCO, volts
Vd	Phase detector output, volts
VCO	Voltage-controlled oscillator
ζ	Damping factor
$\phi = \theta_i - \theta_o$	Phase error in radians
θ_i	Input phase, radians

θ_o	Output phase, radians
t_1, t_2	Time constants of loop filter, sec.
ω	Radian frequency, radians/sec.
ω_n	Loop natural frequency, radians/sec.
ω_o	Center frequency, radians/sec.
$\Delta\omega_h$	Hold-in frequency, radians/sec.
$\Delta\omega_{po}$	Pull-out frequency, radians/sec.

I. INTRODUCTION

There exist in industry today many applications for phase-locked loops. A phase-locked loop is a narrow band filter that continuously tunes itself to the strongest input signal frequency. These tunable filters find their greatest application in space communications where they are used as highly selective, narrow-band noise-rejection filters. Phase-locked loops are used when conventional fixed filters might not stay aligned with the input signal.

Phase-locked loops might be used to "lock on" to a signal which may vary in frequency due to drift or a signal which is frequency or phase modulated. It might also be used to "lock on" to a fixed frequency when components vary due to age and environment.

Phase-locked loops differ from passive filters in that they have active elements and therefore can have a net gain from input to output.

The three main components of phase-locked loops are: a phase detector, a loop filter, and a voltage-controlled oscillator. See Fig. 1.0-1. Prior to stating the objectives of this paper, an understanding of the operation of phase-locked loops is necessary. The

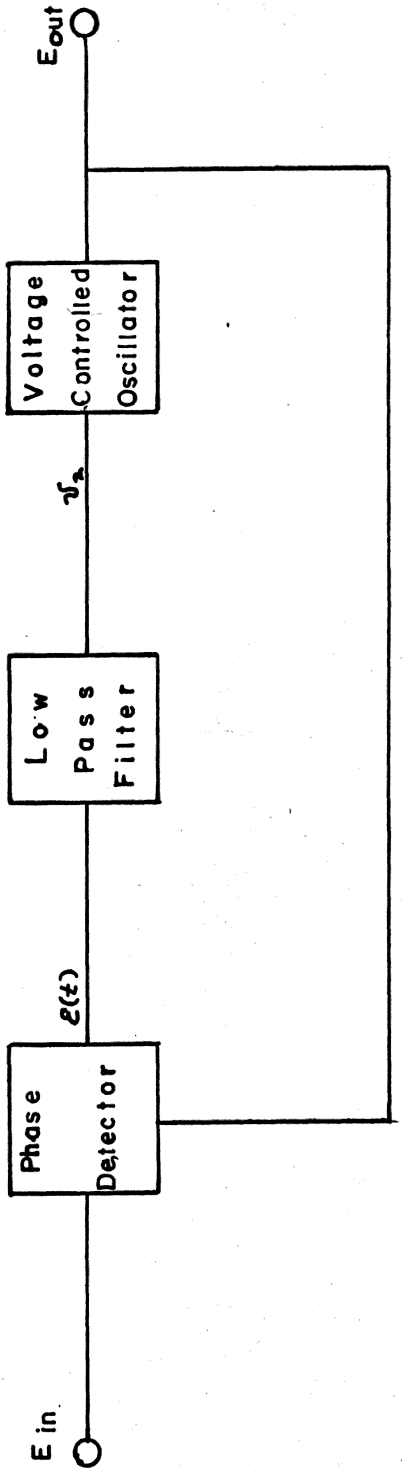

BASIC PHASE-LOCKED LOOP

FIGURE - 1.1-1

over-all system response is shown in Fig. 1.0-2. The functional operation of each part of the system will be outlined briefly.

The phase detector is a device which compares two input signals and provides an output proportional to the phase difference of the signals when the phase difference is small ($< \pi/4$). When the system is out of lock, the difference in frequency between the two signals produces an output which is almost triangular shaped and whose frequency increases with rate of change of phase difference. See Fig. 1.0-3.

The purpose of the low-pass filter is to provide selectivity, and to reject all frequencies except the phase difference information obtained by beating the incoming signal against the local oscillator, but it must also give enough gain at the higher frequencies to allow the loop to pull-in to lock. The low-pass filter establishes the time and frequency response of the loop. The filter can be a simple R C low-pass filter.

The voltage-controlled oscillator (VCO) is the output element, and an error signal at its input produces a corresponding change in the output frequency of the VCO. See Fig. 1.0-4. This oscillator output is

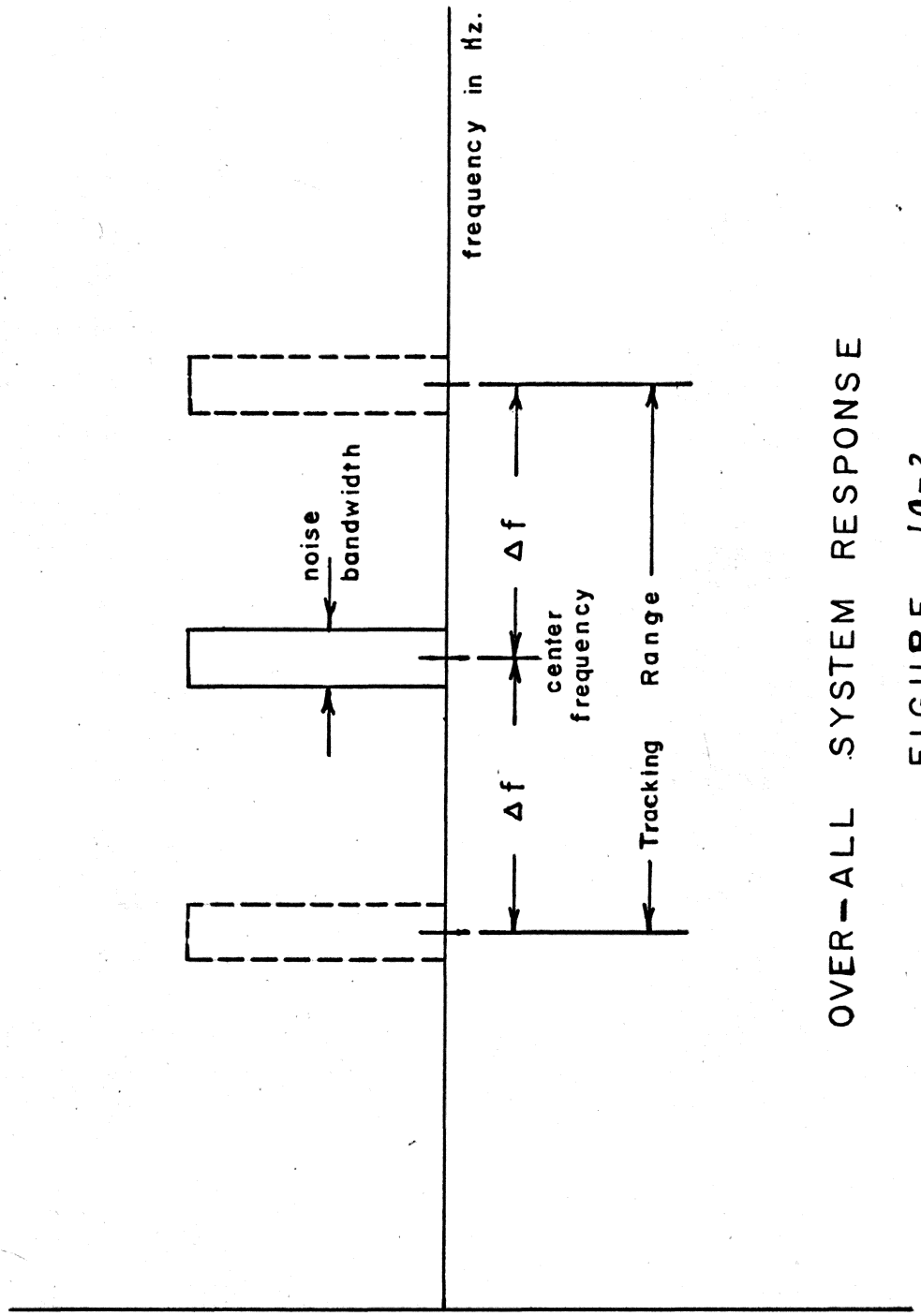

OVER-ALL SYSTEM RESPONSE

FIGURE- 1.0-2

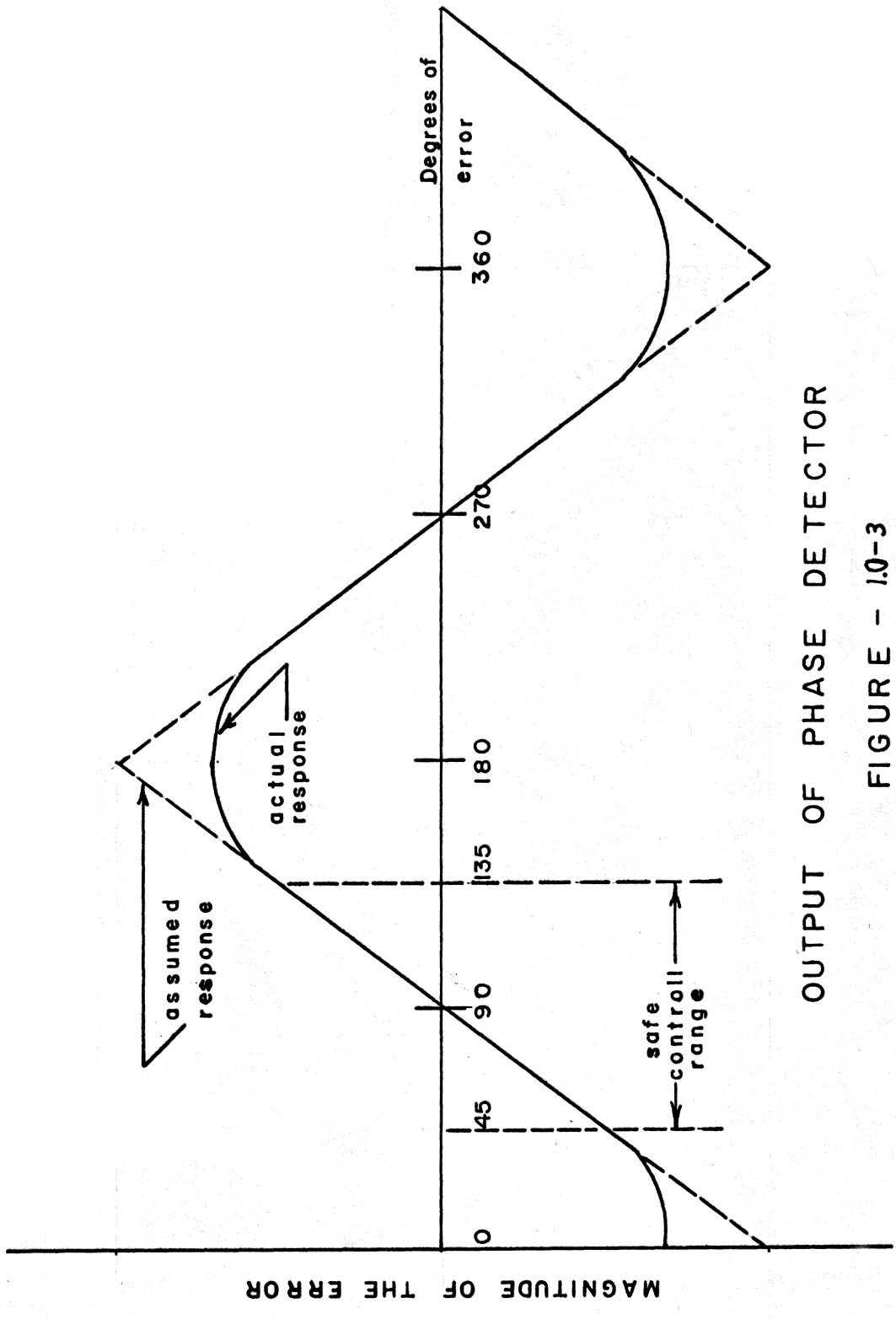

OUTPUT OF PHASE DETECTOR

FIGURE - 1.0-3

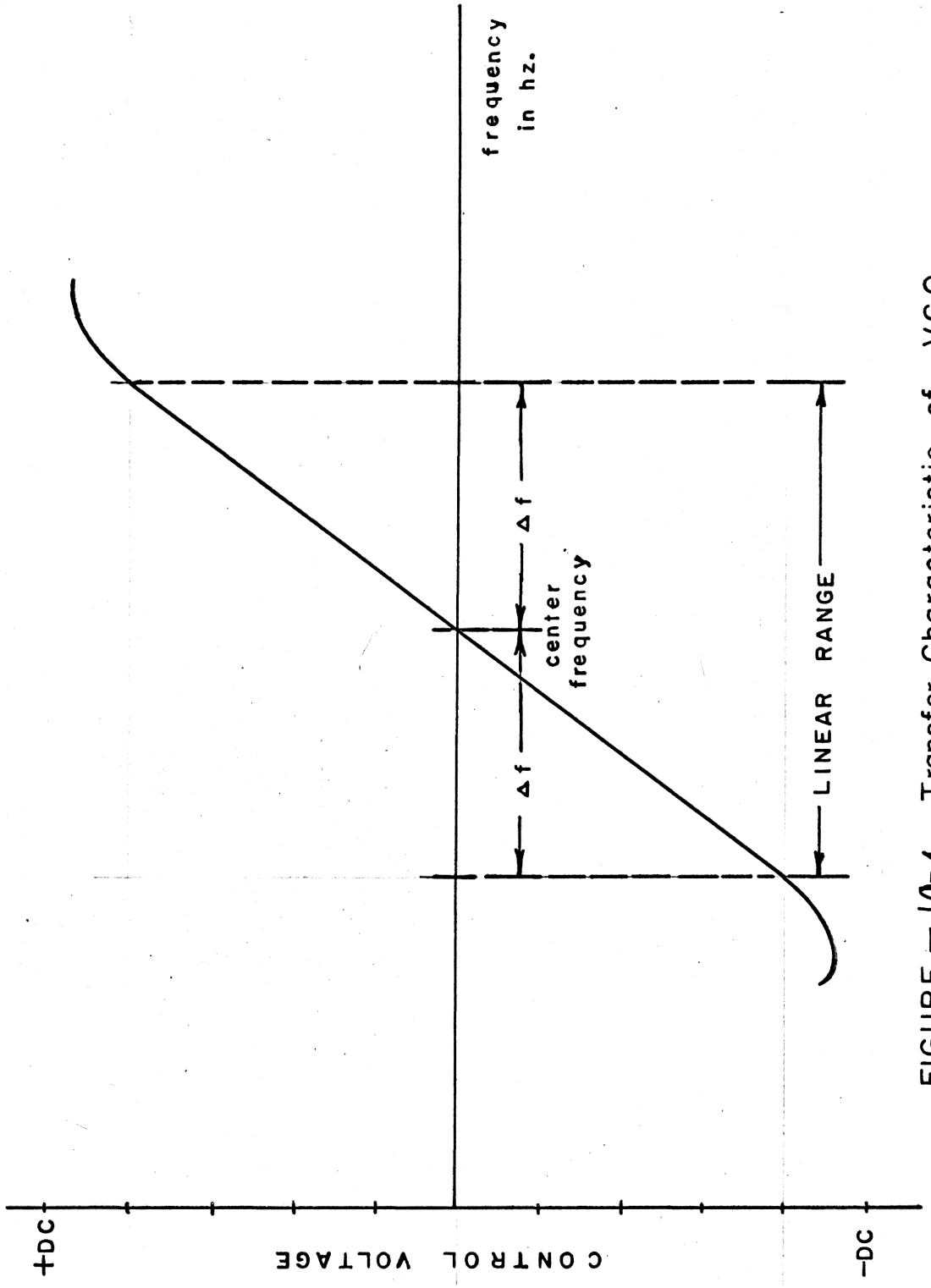

FIGURE — 10-4 Transfer Characteristic of VCO

one of the inputs to the phase detector. The condition for the loop to be in lock is that the incoming and feedback signals be identical in frequency. Under these conditions the phase detector output will be a direct voltage, proportional to the difference in phase.

Because of the nature of the VCO and the phase detector, there will always be varying amounts of phase difference between the output and input as the system tracks the input signal over its range. The VCO needs varying amounts of voltage to alter its frequency, and the phase detector can supply these voltages only at the expense of phase difference.

The phase difference variation should not be great enough to go over the "hump" at $\pm$ 180 degrees as is shown in Fig. 1.0-3 or the system will lose lock. As long as the changes of input frequency remain within the bandwidth of the loop, the system will remain in lock. The servo action between the input and output of the system is the factor which allows the phase-locked loop to track the input.

As mentioned above, the filter establishes the pass band of the system and the noise bandwidth. It is this point that will be of interest in this paper. This paper will investigate the effect of the bandwidth of the

low-pass filter on the pass band of the entire system, the noise bandwidth, time to lock, and noise power in the output.

The procedure will be to conduct a thorough investigation of the literature to determine the theoretical effect of the pass band of the low-pass filter on the entire loop response. The literature review will be followed by an analog simulation of the loop to verify the theoretical results. After the desirability of an automatically tunable low-pass filter has been established, a filter will be built which can automatically adjust its pass band. It will be shown that there is a trade-off between the bandwidth of the pass-locked loop, the speed with which the loop can reacquire lock. A narrow filter bandwidth results in a narrow pass band of the over-all loop, and reduced noise in the output. On the other hand, a narrow pass band means that the phase-locked loop is more likely to come out of lock. The use of a variable-bandwidth filter will, however, find its greatest value in cases where the signal-to-noise ratio is large, as seen in Section 2.6.

II. REVIEW OF PHASE-LOCK-LOOP THEORY

Various aspects of the operation of phase-locked loops have been treated by Gruen[1], Richman[9], Viterbi[14], Jaffe[3], and others. As an introduction to the loop operation the essence of this work will be briefly outlined. The aim of this paper is to derive necessary formulas in terms of the loop parameters and the bandwidth of the low-pass smoothing filter.

The loop transfer function, noise bandwidth, noise power, pull-in range, hold-in range, and the time to lock, as a function of the filter bandwidth, will be developed. The loop transfer function in operational form will be examined and the transient response will be obtained using Laplace transforms. This paper will be concerned primarily with the linear range of the phase detector (small phase errors).

2.1 Transfer Function

It will assumed that our received signal, without noise, has the following form:

$$e_i = \sqrt{2}\, A \sin [\omega_o t + \theta_i(t)] \qquad (2.1\text{-}1)$$

The following additional assumptions are also made:

a. Sinusoidal input proportional to A^2 watts of power.

b. Arbitrary frequency ω_o which is constant.

c. Arbitrary phase θ_i which can be fixed or time varying due to modulation.

d. The loop contains an ideal multiplier.

e. The loop is locked.

The output of VCO is a sinusoid with the frequency controlled by its input voltage:

$$e_{vco} = \sqrt{2}\ B \cos [\omega_o t + \theta_o(t)] \qquad (2.1\text{-}2)$$

The error voltage $\varepsilon(t)$, which is the product of the output of the VCO and the input signal, is:

$$\varepsilon(t) = (e_i)(e_{vco})\ K_{pd} \qquad (2.1\text{-}3)$$

where K_{pd} is the gain constant associated with the phase detector. The expression for error voltage contains a term which is proportional to the difference in the phase of the input and the output, and a term which is proportional to twice the carrier frequency. If it is assumed that the low-pass filter effectively rejects the double-frequency terms, it can be shown that the error voltage ε (t) has the following form:

$$\varepsilon(t) = ABK_{pd} \sin [\theta_1(t) - \theta_o(t)] \qquad (2.1\text{-}4)$$

where K_{pd} is the phase detector gain constant. At this point no generality is lost by assuming A and B equal to one. In the range near lock the phase detector is approximately linear, therefore:

$$\varepsilon(t) = K_{pd} \sin [\theta_1(t) - \theta_o(t)] \qquad (2.1\text{-}5)$$

The error voltage is transmitted through the low-pass filter whose transfer function is F(s). This provides $v_2(t)$ which is applied to the VCO to control its frequency. The deviation of the frequency of the VCO from its free running or natural frequency is:

$$w_o(t) = K_{vco}\, v_2(t) \qquad (2.1\text{-}6)$$

where it is assumed that the VCO frequency is a linear function of $v_2(t)$ as shown in Fig. 1.0-4 and K_{vco} is the constant of proportionality equal to the gain in radians/sec./volt. By taking the Laplace transform of equation 2.1-6, we obtain

$$\mathcal{L}[\theta_o(t)] = s\theta_o(s) - \theta_o(0^+) = K_{vco}\, v_2(s) \qquad (2.1\text{-}7)$$

therefore,

$$\theta_o(s) = \frac{K_{vco}\, v_2(s)}{s} \qquad (2.1\text{-}8)$$

The voltage $v_2(t)$ is given by:

$$v_2(t) = \mathcal{L}^{-1}\left\{F(s) \cdot [\varepsilon(t)]\right\} \qquad (2.1\text{-}9)$$

Eqn. 2.1-8 shows that the output phase is proportional to the integral of the control voltage.

Using Laplace notation and combining Eqns. 2.1-5, 2.1-7, and 2.1-8 the loop transfer equation is:

$$\frac{\theta_o(s)}{\theta_i(s)} = H(s) = \frac{KF(s)}{s + KF(s)} \qquad (2.1\text{-}10)$$

where $K = K_{vco} \cdot K_{pd}$ is the loop gain constant in radians per second and F(s) is the transfer function of the low-pass filter. The loop filter and its transfer function will now be considered. It has been shown by Jaffe and Rechtin[3] that the optimum filter function differs with the type of input. The optimum filter was derived by making the transient error plus the noise error a minimum. They assumed white noise and three different types of modulation at the input and the results are summarized in Table 2.1-1. The operational form of F(s) is of importance here and not the definition of the terms represented in F(s) given.

The filter for case A as defined in Table 2.1-1 is easy to realize because it represents a simple

TABLE —2.1-1

Optimum Functions

Case	Optimum H(s)	F(s)
A. Phase Step	$\frac{W_1}{S + W_1}$	$\frac{W_1}{K_{vco}\ K_{pd}}$
B. Frequency Step	$\frac{W_n^2 + \sqrt{2}\, W_n S}{W_n^2 + \sqrt{2}\, W_n S + S^2}$	$\frac{W_n^2 + \sqrt{2}\, W_n S}{K_{vco}\ K_{pd}\ S}$
C. Frequency Ramp	$\frac{W_3^3 + 2 W_3^2 S + 2 W_3 S^2}{W_3^3 + 2 W_3^2 S + 2 W_3 S^2 + S^3}$	$\frac{W_3^3 + 2 W_3^2 S + 2 W_3 S^2}{K_{vco}\ K_{pd}\ S^2}$

resistive network and is of little interest because the response to disturbances is poor. The prime disadvantage is, however, that the resistive network provides a first-order loop, whose loop gain constant cannot be chosen independently from the frequency response of the loop.

The filter for case C as defined in Table 2.1-1 is very difficult to realize and can be approximated by:

$$F(s) = \frac{(st_1 + 1)(st_3 + 1)}{(st_2 + 1)(st_4 + 1)} \qquad (2.1\text{-}11)$$

which yields a third-order loop.

Case B is the filter function as defined in Table 2.1-1 that is most commonly used and is approximated by the networks shown in Fig. 2.1-1. Case B is approximated by the transfer function:

$$F(s) = \frac{t_1 s + 1}{t_2 s + 1} \qquad (2.1\text{-}12)$$

Cases A and C will not be investigated and only occasional remarks concerning them will be made for purposes of comparison with the second-order loop obtained with case B.

Two filters which are used widely are shown in Fig. 2.1-1, along with their transfer functions. The passive filter is simple to construct and is adequate in mose cases. The active filter makes use of an operational amplifier to achieve the desired transfer characteristic.

Adopting the notation of linear servomechanisms[4], the loop transfer function can be shown to be:

$$\text{(a)}\quad H(s) = \frac{[2\zeta\omega_n - \omega_n^2/K]\, s + \omega_n^2}{s^2 + 2\zeta\omega_n s + \omega_n^2} \qquad (2.1\text{-}13)$$

$$\text{(b)}\quad H(s) = \frac{2\zeta\omega_n s + \omega_n^2}{s^2 + 2\zeta\omega_n s + \omega_n^2} \qquad (2.1\text{-}14)$$

for the passive and active filters, respectively, and the natural frequency ω_n and damping factor ζ are defined as follows:

(a) Passive filter

$$\omega_n = \sqrt{K/t_2} \qquad \zeta = \frac{1 + Kt_1}{2\omega_n t_2} \qquad (2.1\text{-}15)$$

(b) Active filter

$$\omega_n = \sqrt{K/t_1} \qquad \zeta = t_2/2\sqrt{K/t_1} \qquad (2.1\text{-}16)$$

FIGURE 2.1-1 Filters Widely Used

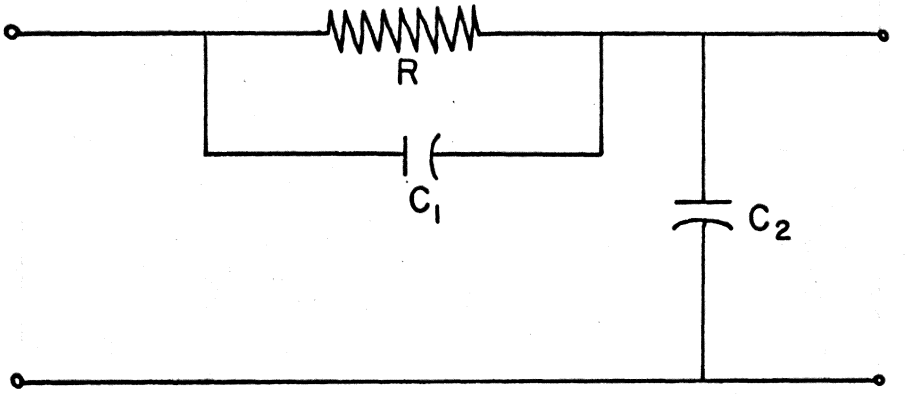

$$F(s)=\frac{SRC_1+1}{SR(C_1+C_2)+1}=\frac{t_1s+1}{t_2s+1}$$

PASSIVE FILTER

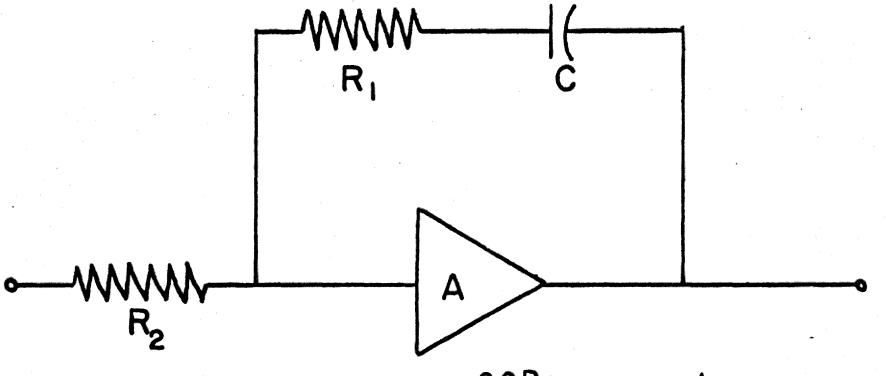

$$F(s)=\frac{SCR_2}{SCR_1+1}=\frac{t_1s}{t_2s+1}$$

ACTIVE FILTER

The terms t_1 and t_2 are as defined in Fig. 2.1-1. It is interesting to note that for the active filter, only the damping factor is affected by the filter bandwidth. The remainder of this paper will be concerned with the passive filter.

Fig. 2.1-2 shows the effect of the filter pass band on the over-all pass band of the loop. Eqn. 2.1-13 was used and the low-pass filter was allowed to take on pass bands of 1, 5, 10, 500, and 1000 Hz.

2.2 Hold-in Range

The nonlinear differential equation for the operation of a second-order loop is:

$$\ddot{\phi}(t) + \left[\frac{1}{t_2} + \frac{Kt_1}{t_2} \cos \phi(t)\right]\dot{\phi} + \frac{K}{t_2} \sin \phi(t) = \ddot{\theta}_i(t) + \frac{1}{t_2} \dot{\theta}_i(t) \qquad (2.2\text{-}1)$$

The equation can be solved by graphical phase plane techniques. Fig. 2.2-1 is the solution of the above equation. The phase plane plot has the derivative of the phase error (the frequency error) plotted versus the phase error. If the initial frequency and phase errors place the system above line B-B which is called the limit cycle, the frequency error tends to increase

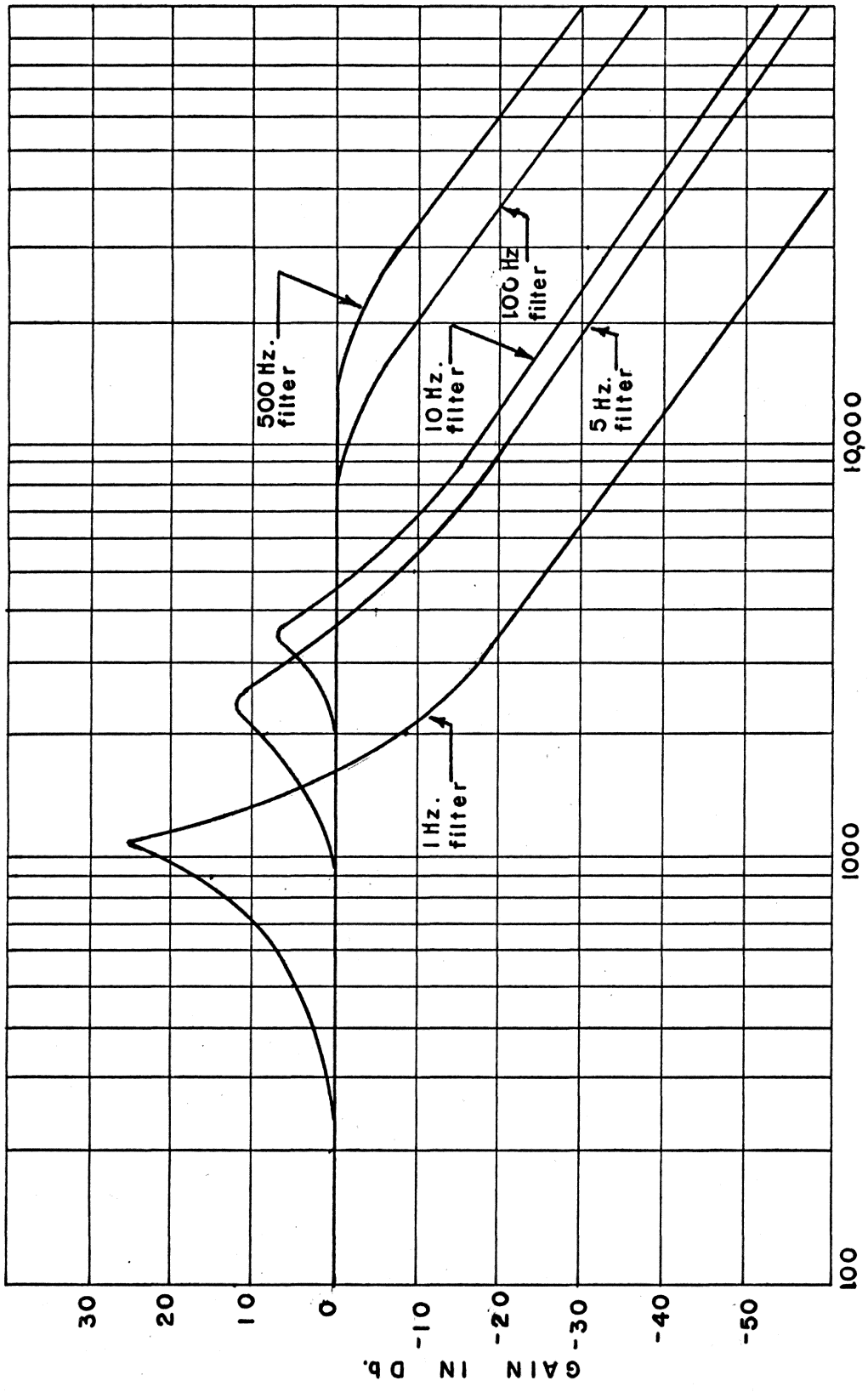

FIGURE 2.1-2 Frequency Response of Loop

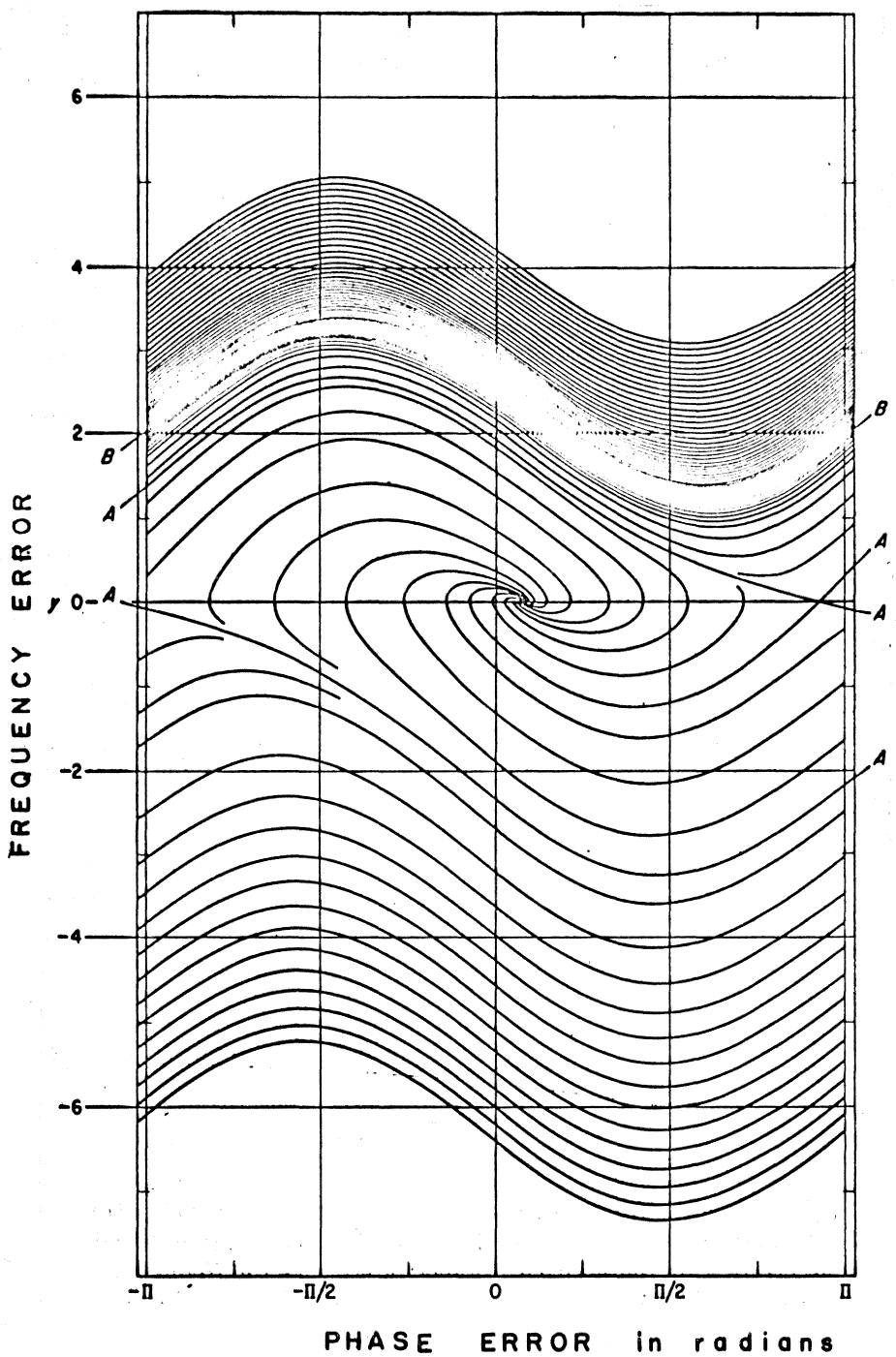

FIG. 2.2-1 Phase-Plane Solution for PLL

and phase lock is never achieved. If the initial position is below this line, the system achieves phase lock. Line B-B separates trackable and nontrackable signals. When the phase-locked loop operates with an instantaneous phase error lying in the positive slope range of its error characteristic, it is considered to be "in lock." When the instantaneous phase error exceeds approximately $\pm \pi/2$ radians, the phase tracking becomes unstable because the feedback becomes positive, during which time the system is "out of lock." Noting that a limit cycle represents an undesirable mode of operation of the phase-locked loop, it is important to be able to determine the maximum allowable mistuning to insure operation below the limit cycle.

Hold-in range will be defined as that value of frequency step below which the loop does not skip cycles but remains in lock. To investigate the hold-in characteristic of phase-locked loops, one must first examine the phase error, $\phi = \theta_i - \theta_o$ that results from a specified input. It can be shown that the error in a locked loop is given by:

$$\phi(s) = \frac{s\,\theta_i(s)}{s + F(s)\,K} \qquad (2.2\text{-}2)$$

The steady-state error is easy to analyze with the use of the final value theorem[12] from Laplace transforms theory, which is:

$$\lim_{t \to \infty} \phi(t) = \lim_{s \to o} s\,\phi(s) \tag{2.2-3}$$

For a step of phase, $\theta(s) = \frac{\Delta\theta}{s}$, the final value theorem yields a zero steady-state error. For a step frequency input of magnitude $\Delta\omega$, $\theta_i(s) = \frac{\Delta\omega}{s^2}$, the final value theorem yields a steady-state error of:

$$\lim_{s \to o} \frac{\Delta\omega}{s + KF(s)} = \frac{\Delta\omega}{KF(o)} \tag{2.2-4}$$

Drawing once again from servomechanism theory, the product KF(o) is called the "velocity constant" and is denoted as K_v. K_v for the passive filter is equal to the loop gain constant K because F(o) is equal to one; however, for the active filter, K_v is equal to KA where A is the gain of the operational amplifier. This tends to indicate that the active filter might trace a frequency step better than the passive filter; however, if a high gain amplifier were inserted in series with the passive filter, the same results would be obtained. One may conclude that a large loop gain constant will

result in a small steady-state velocity error. Values of 10^5 are common as will be shown later.

At the limits of the hold-in range (for a phase error approaching $\pm \pi/2$, the linear approximation does not hold for the response of the phase detector, and it can be shown that the true expression for a phase detector with sinusoidal characteristic is:

$$\sin \phi = \frac{\Delta \omega}{K_v} \tag{2.2-5}$$

Therefore, since sin ϕ cannot exceed $\pm$ 1,

$$\Delta \omega_h = \pm K_v \tag{2.2-6}$$

is sometimes defined as the hold-in range. This equation says that the hold-in range can be made arbitrarily large, although in reality it is limited by the phase detector range, saturation of amplifiers, and limited control range of the VCO.

The above result is the steady-state error limit, but the transient (or short term) error can pull the loop out of lock even if the steady-state error is within the hold-in range.

Viterbi[13] arrived at an expression for hold-in experimentally in terms of the natural resonant

frequency ω_n with a damping factor between 0.4 and 1.4. The equation is:

$$\Delta\omega_h = 1.8\,\omega_n\,(\zeta + 1) \qquad (2.2\text{-}7)$$

If a step of frequency is less then the transient error will be such that the loop will remain in lock. If $\Delta\omega$ is greater than $\Delta\omega_h$ then the loop will skip cycles before locking.

2.3 Pull-in Range

When the system is out of lock, the usual filter is such that the sum frequency component out of the phase detector is greatly attenuated, and the oscillator output is very nearly sinusoidal. It is, nevertheless, slightly distorted, one half-cycle taking less time than another with the results being that the mean value is not zero. This is due to the fact that the VCO output is being frequency modulated at the difference frequency. The second-order loop filter contains an integrator in its loop. This integrator builds up an increasing output in response to a direct voltage input. This waveform with increasing d-c offset is applied to the VCO. The VCO output frequency will change in response to the d-c level at its input and if the change is sufficient to

reduce the error, lock-in will eventually result. It is possible to calculate the magnitude of this error voltage by integrating an expression for the error so as to determine its mean value. The maximum pull-in range of the system then follows when this bias voltage is compared with the control sensitivity of the oscillator.

This approach was used by Richman[9] to determine a formula for the pull-in range, and experimental data provided by Gruen[1] indicates Richman's results to be reasonable for high gain loops. Richman's formula for pull-in frequency is:

$$\Delta\omega_p = K\sqrt{\frac{2t_1}{t_2} - \left(\frac{t_1}{t_2}\right)^2} \qquad (2.3\text{-}1)$$

which reduces to a simpler expression for most filters:

$$\Delta\omega_p \approx K\sqrt{\frac{2t_1}{t_2}} \qquad (t_1 < t_2) \qquad (2.3\text{-}2)$$

Fig. 2.3-1 is a plot of Eqn. 2.3-2 and it demonstrates the improvement in the pull-in range that can be achieved if the bandwidth of the low-pass filter could be made large when the loop is out of lock.

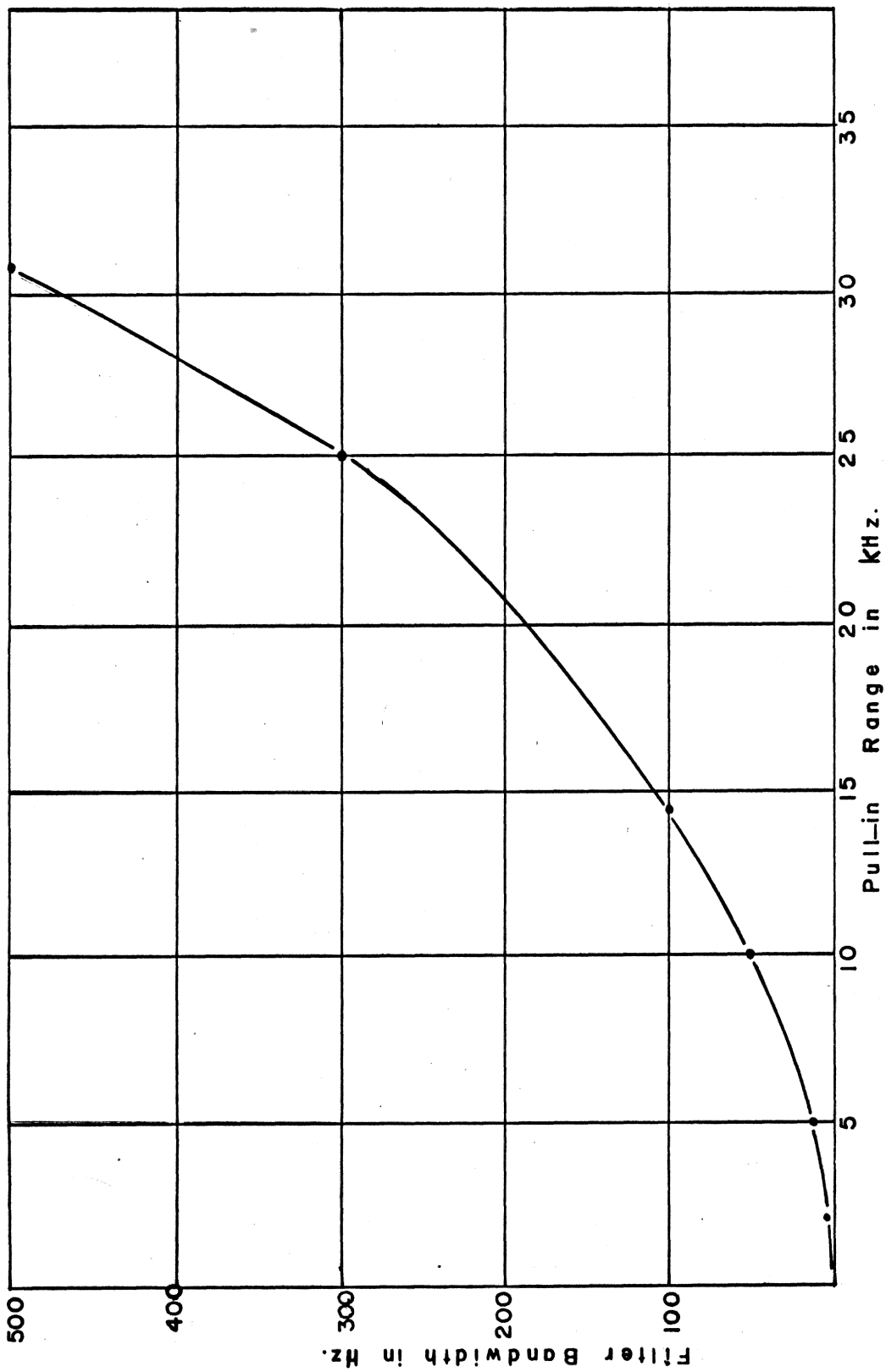

FIGURE 2.3-1 Pull-in Characteristic of Loop

2.4 Noise Bandwidth

In the presence of noise the input voltage can be expressed as:

$$e_i(t) = \sqrt{2}\, A \sin [\omega_o t + \theta_i(t)] + \eta(t) \qquad (2.4\text{-}1)$$

The propagation of signal phase modulation and random noise through the network is assumed to be independent. This is equivalent to saying that the superposition principle holds. Although the loop is not linear, experimental results have shown that the independence above is a good approximation.

The received noise is assumed to be a stationary gaussian distributed voltage given by:

$$\eta(t) = \sqrt{2}\, \lambda_1(t) \cos\omega_o t + \sqrt{2}\, \lambda_2(t) \sin\omega_o t \qquad (2.4\text{-}2)$$

where $\eta(t)$ represents the amplitude of the random noise in a narrow frequency band centered on ω_o. $\lambda_1(t)$ and $\lambda_2(t)$ are uncorrelated gaussian distributed processes independent of frequency, which represent the quadrature and inphase components. $\eta(t)$ being stationary means that all statistical properties are

constant for all time. A gaussian function implies a zero mean function.

The loop noise bandwidth B_L is defined[5] as:

$$B_L = \frac{1}{H(j\omega)}_{max} \int_{-\infty}^{\infty} H(j\omega)^2 \, d\omega \qquad (2.4\text{-}3)$$

Substituting in the transfer function from Eq. 2.1-13 and performing the indicated integration which has been tabulated in the appeodix of Theory of Servomechanisms[17], for a number of transfer functions, the bandwidth can be shown to be:

$$B_L = \frac{4\zeta^2 - 4\zeta\omega_n/K + (\omega_n/K)^2 + 1}{2\zeta} \pi\omega_n \qquad (2.4\text{-}4)$$

By substituting the expressions for ω_n and ζ it can be shown that:

$$B_L = \frac{K\pi}{t_2} \frac{Kt_1^2 + t_2}{Kt_1 + 1} \qquad (2.4\text{-}5)$$

If it is assumed that $Kt_1 \gg 1$ and $Kt_1^2 \gg t_2$ then:

$$B_L = \frac{K\pi t_1}{t_2} \qquad (2.4\text{-}6)$$

Noting here that, in all the expressions in this section and the sections concerning noise which follow, it was assumed that the noise contributed by the loop itself is negligible compared to the input noise and therefore has not been included. This is a good assumption in most cases because the phase-locked loop usually follows IF stages of a receiver for example, and most of the noise is contributed by early stages of amplification. This is equivalent to saying that the noise figure for the loop is nearly unity.

Fig. 2.4-1 is a plot of Eq. 2.4-6 as a function of the filter bandwidth (t_2) and it demonstrates the fact that a narrow loop filter is necessary in order that the noise at the output be minimized.

2.5 Signal-to-Noise Ratio

Viterbi[13] defined the loop signal-to-noise ratio as:

$$SNR_L = \frac{(SNR)_i \; B_i}{B_L} \qquad (2.5\text{-}1)$$

where B_i is the bandwidth of the input noise and SNR_i is the input signal-to-noise ratio. If the expression for B_L is substituted in, then:

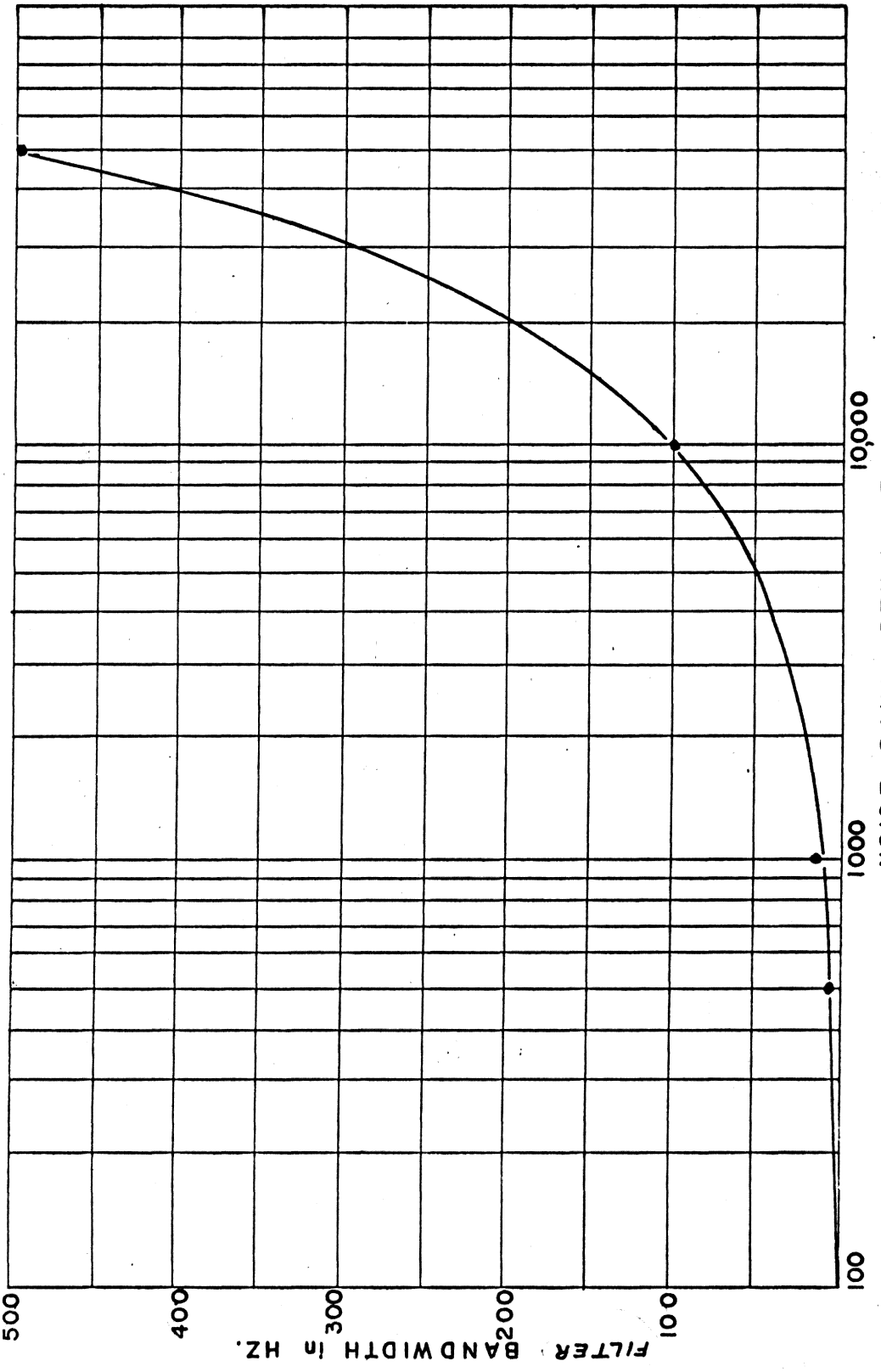

FIGURE 2.4-1 Noise Bandwidth Vs Filter Bandwidth

$$SNR_L = \frac{(SNR)_1 \, B_i \, t_2}{Kt_1} \qquad (2.5\text{-}2)$$

We can conclude that the SNR_L will be improved as the bandwidth of the filter is made small.

2.6 Threshold Noise

Phase error in the presence of noise is a statistical quantity and is usually described by its rms value. However, the instantaneous value of the error due to noise peaks can greatly exceed the rms value.

Many authors have tried to develop exact expressions for noise threshold. However, due to the complexity of handling the nonlinearity and the statistical quantity involved, they have been forced to make approximations which fit the particular case they were investigating.

Threshold is defined as that minimum value of signal-to-noise ratio at which the loop can acquire lock. We would expect that as the signal-to-noise ratio decreases, a limit is reached at which the loop cannot acquire lock. Experimental results of Viterbi[13] indicate that lock cannot be maintained below a loop signal-to-noise ratio of one, and that acquisition is nearly impossible below a loop signal-to-noise ratio of two. The acquisition minimum is then of primary

importance in design because if a loop cannot acquire lock, it most certainly cannot maintain lock.

If the expression for the variance of the output noise as given by Eq. 2.5-4 is examined it can be shown that the output phase jitter increases as the loop noise-bandwidth increases. It can be concluded that increasing the bandwidth of the filter, which in turn increases the loop noise bandwidth, would have a detrimental effect. This would lead to the conclusion that in a noisy environment any attempt at increasing the loop filter bandwidth would increase the chance of losing lock due to noise, and decrease the chance of acquiring lock.

2.7 Time to Lock

Viterbi[14] derived approximate value for the time required for a loop to pull-in to lock for some initial frequency offset $\Delta\omega$. Viterbi used the following expression:

$$t_p = \int_{\phi_1}^{\phi_2} \frac{d\phi}{\dot{\phi}} \qquad (2.7\text{-}1)$$

and assuming the linear approximation carried out the integration arriving at an approximate expression for the time as:

$$t_p = \frac{(\Delta\omega)^2}{2\zeta\omega_n^3} \qquad (2.7\text{-}2)$$

Due to the linear approximation, the equation should not be used for near the hold-in range. If the expressions for ω_n and ζ are substituted into Eq. 2.8-2, it can be shown that:

$$t_p = \frac{(\Delta\omega)^2\ t_2^2}{K\ (1 + Kt_1)} \qquad (2.7\text{-}3)$$

It can be concluded that increasing the bandwidth of the filter very rapidly decreases the time required to lock for a step of frequency.

For a step of phase ($\Delta\theta$) it will be shown that the transients will decay as an exponential with five time constants approximately equal to:

$$t_p \approx \frac{5\ t_2}{Kt_1} \qquad (2.7\text{-}4)$$

The same conclusions as above can again be made.

III. TRANSIENT RESPONSE OF LOCKED LOOP

The transient response of the locked loop will be investigated in detail in the sections which follow. The expression for the response of the locked loop will be determined from Laplace transform theory for a step phase and a step frequency input. The response of the loop will be determined for each of the three cases of damping factor. The transient analysis will be followed by a study of the root-locus to determine the stability of the loop and the effect of varying the pass band of the low-pass filter on the loop stability. The phase-locked loop will then be simulated in order to verify the transient response of the loop.

3.1 Analysis

The transfer function H(s) given by Eqn. 2.1-13 can be used to determine the transient response of the loop to a step phase shift and a step frequency shift. Three damping conditions are possible and each response will be determined. The transfer function can be put in the following form in order to simplify the inverse Laplace transform:

see 2.1-13

$$H(s) = \frac{A\,(s + a)}{s^2 + 2\zeta\omega_n s + \omega_n^2} \qquad (3.1\text{-}1)$$

Table 3.1-1 summarizes the results of the inverse Laplace transforms. The table shows only the transients and we can easily observe that each of the transients is controlled by the damping constant or the natural resonant frequency or both. The damping constant of the system is:

$$\zeta = \frac{1 + K t_1}{2\omega_n t_2} \qquad (3.1\text{-}2)$$

A value of ζ between 0.5 and 1.0 is usually large enough to prevent excessive oscillation and small enough to avoid excessive sluggishness. The frequency of the system at which it would oscillate in the absence of damping is:

$$\omega_n = \sqrt{K/t_2} \qquad (3.1\text{-}3)$$

If we now examine the time response of the loop, one can see that as t_2 is made small (equivalent to enlarging the pass band of the low-pass filter) the transients will die out more rapidly. Therefore, a wide bandwidth filter is desirable in order to minimize the time response of the loop.

DAMPING	PHASE STEP	FREQUENCY STEP
$\zeta < 1$	$e^{-\zeta\omega_n t}\left[\cos\sqrt{1-\zeta^2}\,\omega_n t - \frac{\zeta}{\sqrt{1-\zeta^2}}\,\sin\sqrt{1-\zeta^2}\,\omega_n t\right]$	$\frac{1}{\omega_n} e^{-\zeta\omega_n t}\left[\frac{1}{\sqrt{1-\zeta^2}}\,\sin\sqrt{1-\zeta^2}\,\omega_n t\right]$
$\zeta = 1$	$e^{-\omega_n t}\left[1-\omega_n t\right]$	$t\,e^{-\omega_n t}$
$\zeta > 1$	$e^{-\zeta\omega_n t}\left[\cosh\sqrt{\zeta^2-1}\,\omega_n t - \frac{\zeta}{\sqrt{\zeta^2-1}}\,\sinh\sqrt{\zeta^2-1}\,\omega_n t\right]$	$\frac{e^{-\zeta\omega_n t}}{\omega_n}\left[\frac{1}{\sqrt{\zeta^2-1}}\,\sinh\sqrt{\zeta^2-1}\,\omega_n t\right]$

TABLE— 3.1-1 Transient Phase Error for Second—Order Loop

3.2 Root-Locus Presentation

A great deal of insight into the behavior of a phase-locked loop can be obtained from the root-locus presentation of the transfer function. If the transfer function given by Eq. 2.1-13 is used, and the system is treated as a second-order servo loop, the root-locus shown in Fig. 3.2-1 can be obtained. In this case, the loop gain is allowed to vary from zero to infinity. Initially, the roots move toward each other along the negative real axis. In this region, the system is overdamped. When they meet, the system becomes critically damped. They then split into a complex conjugate pair and the system is underdamped. With sufficiently high gain, the locus eventually returns to the real axis due to the finite zero and the system is overdamped again. One branch of the locus terminates at the finite zero; the other terminates at infinity.

Because the root-locus remains in the left-half plane for all values of K, the system is unconditionally stable. This is not true for the third-order loop because, at low values of loop gain, the root-locus goes into the right-half plane and the system becomes unstable. When a third-order loop is used, the gain

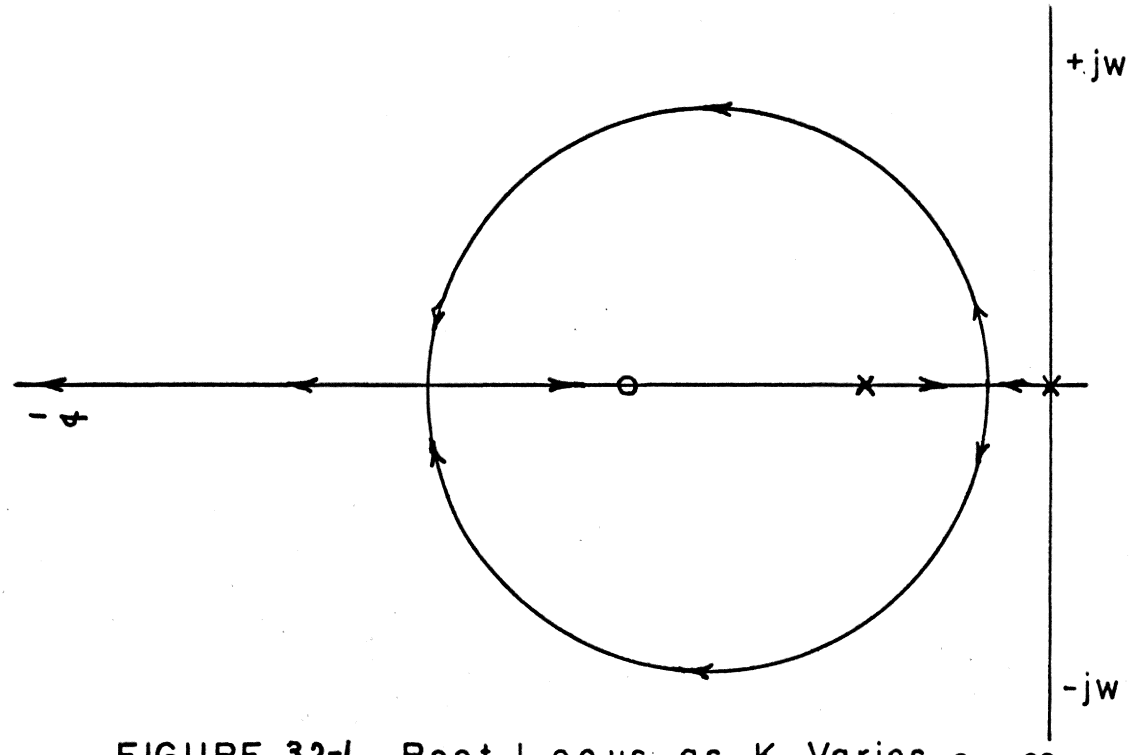

FIGURE 3.2-1 Root Locus as K Varies $0 \rightarrow \infty$

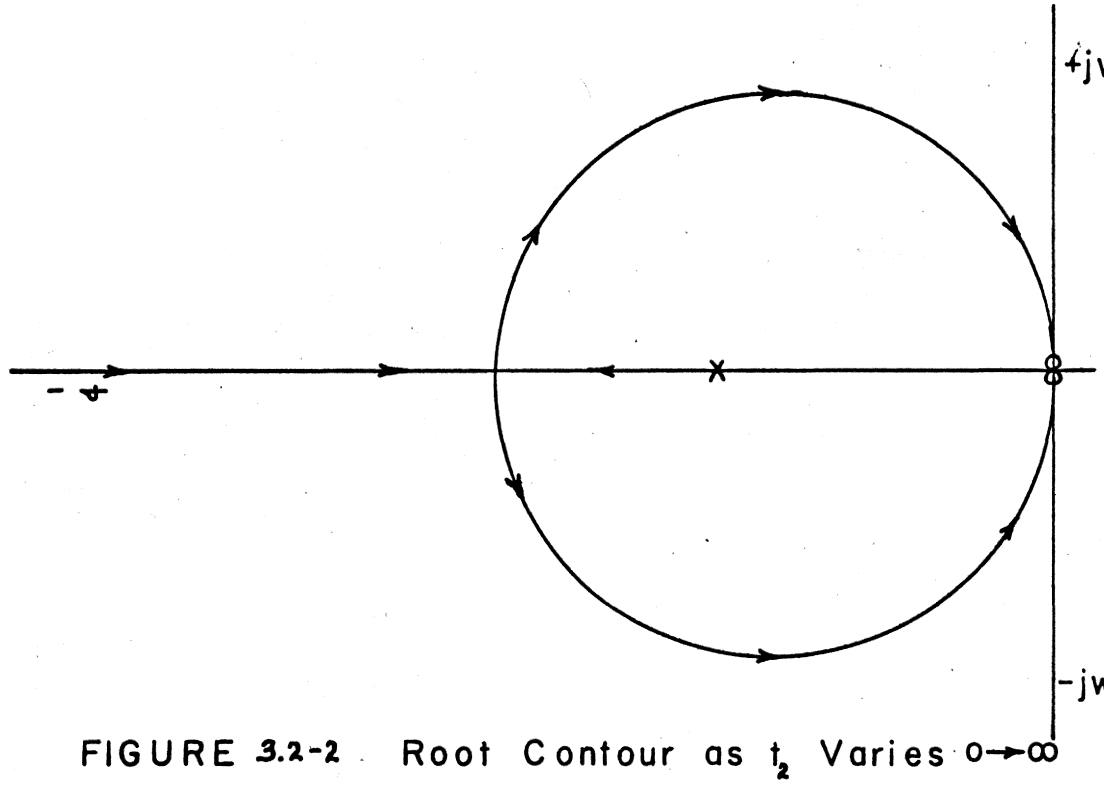

FIGURE 3.2-2 Root Contour as t_2 Varies $0 \rightarrow \infty$

must be large enough to prevent the root-locus from crossing into the right-half plane.

To investigate the effect of varying the bandwidth of the filter, the root-contour plot must be obtained. The root-contour plot allows one to observe the effect of varying a pole from zero to infinity. Fig. 3.2-2 is the root-contour plot of the phase-locked loop, when the filter pass band is allowed to vary from zero to infinity. It can be observed that the same general statements apply here as they did for the root-locus.

3.3 Analog Simulation

The time response of the system to a step phase and a step frequency shift will now be verified. Note here, that the analog approach taken is a simulation of the loop and not a solution of the differential equations for the response.

Fig. 3.3-1 represents the system in block diagram without noise. If tests with noise present at the input are desirable, it can be shown that the following equation is applicable:

$$\phi(t) = \theta_i(t) - \frac{F(s)\,K}{s}\,[AB \sin \phi(t) + \eta(t)] \qquad (3.3\text{-}1)$$

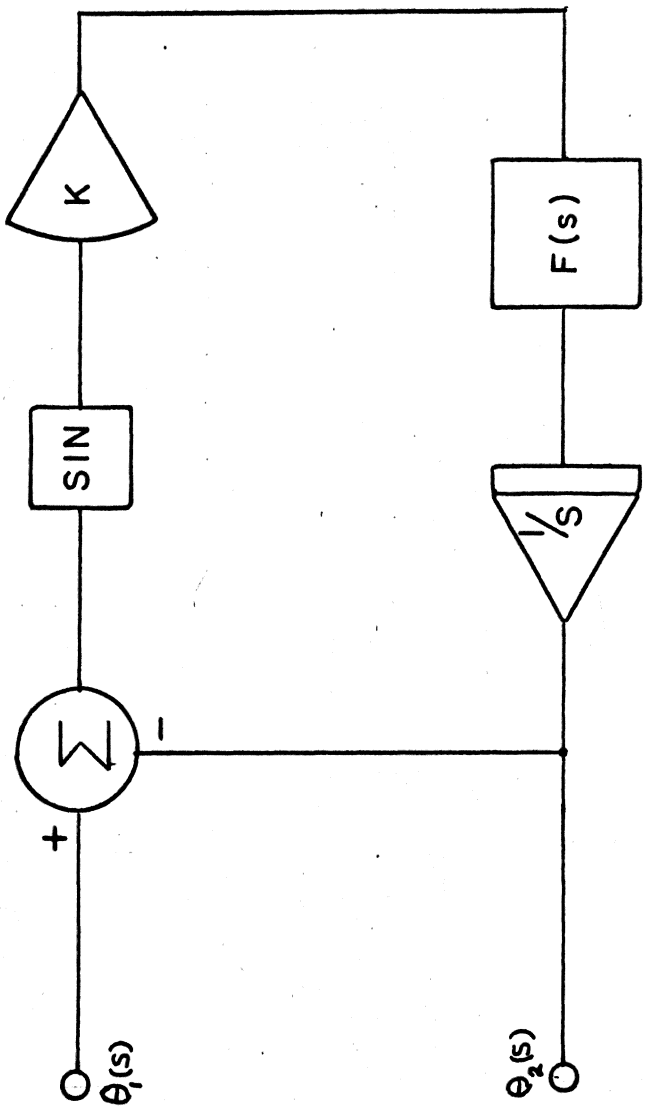

FIGURE 3.3-1 Non-linearized Loop Without Noise

For small values of error, $\phi(t)$, Fig. 3.3-2 is applicable.

From Fig. 3.3-1, the phase detector in the linearized model becomes a simple summer. The voltage-controlled oscillator becomes an integrator with a transfer function:

$$H(s) = 1/s \tag{3.3-2}$$

The actual sensitivities of the VCO and the phase detector have been included in the loop gain constant, K.

The filter must be simulated in a manner which leaves the break frequencies available for adjustment. Given the transfer function:

$$E_o/E_{in} = \frac{t_1 s + 1}{t_2 s + 1} \tag{3.3-3}$$

The equation may be rearranged to obtain:

$$E_o = 1/t_2 \left[t_1 E_{in} + E_{in}/s - E_o/s\right] \tag{3.3-4}$$

If this equation is now modeled using operational blocks, the transfer function of the filter with the break frequencies is available as simple potentiometer settings. Fig. 3.3-3 shows the analog

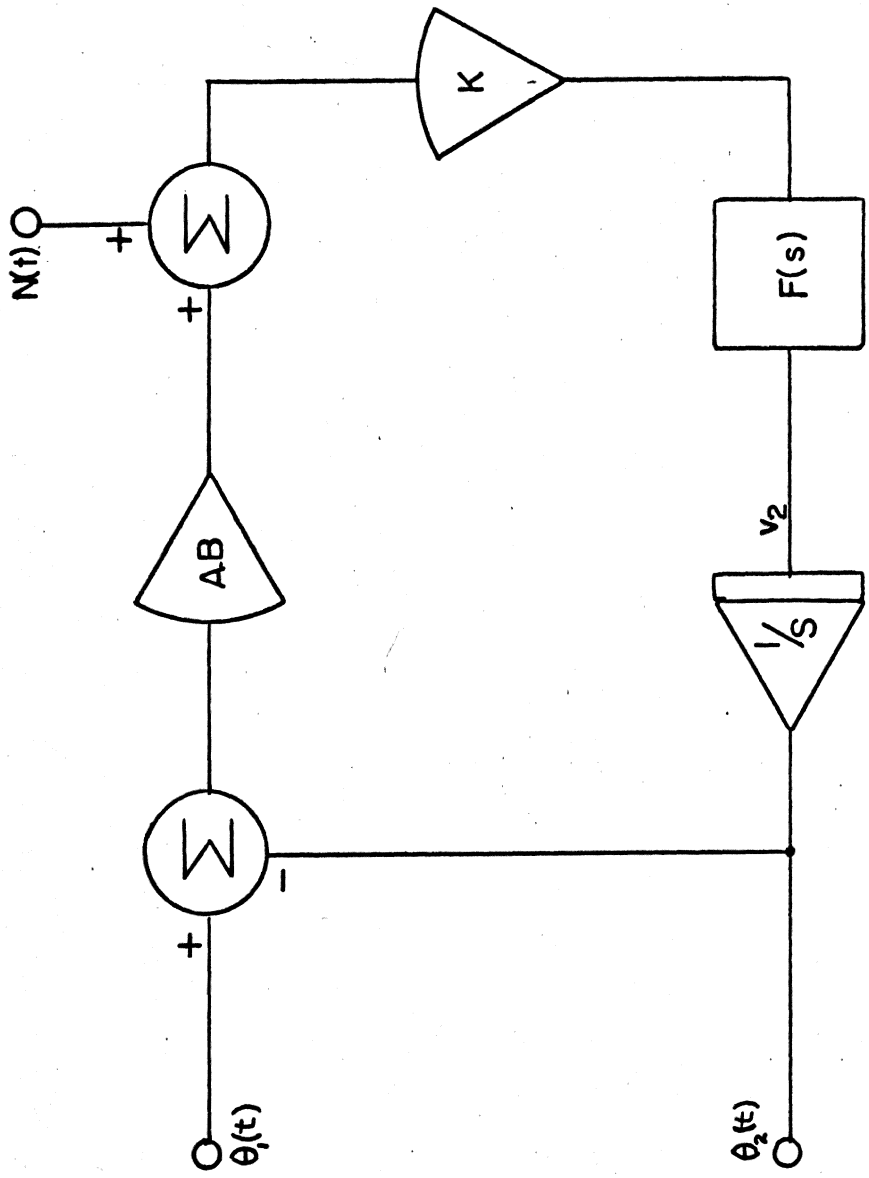

FIGURE 3.3-2 Linearized Loop With Noise

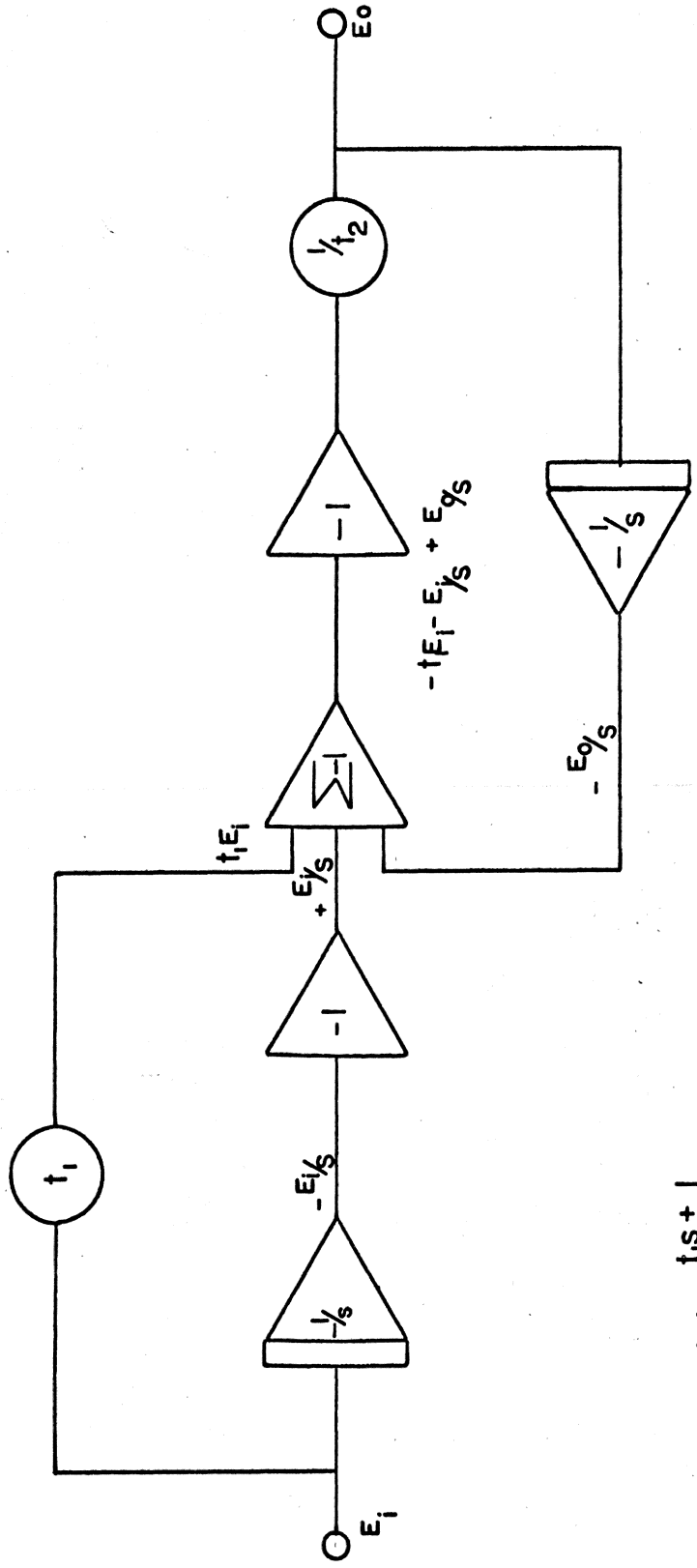

$$F(s)=\frac{t_1 s+1}{t_2 s+1}$$

FIGURE—3.3-3 Low—Pass Filter Simulation

computer program which represents the filter transfer function in the form given in Eqn. 3.3-3. The analog computer scaled program is shown in Fig. 3.3-4. The non-linearity of the phase detector was not included in the analog program due to not having a sin function operator available. Therefore, this analysis must be limited to cases such that phase error steps are small enough that the sin of the error is approximately equal to the error itself. The first thing that is desirable is to investigate the effect of varying the bandwidth of the filter on the response of the loop to a step phase shift and a step frequency shift.

The following example problem will be used: The VCO tracking range will be assumed to be approximately 5000 Hz. The approximate loop gain necessary to insure a steady-state error not to exceed 10 degrees is given by Eqn. 2.2-5 which can be solved for K:

$$K = \frac{\Delta\omega}{\sin \phi} \qquad (3.3\text{-}5)$$

The loop gain constant will be assumed to be 2×10^5 radians per second.

Tests will be made using five different bandwidth filters which are 1 Hz, 5 Hz, 10 Hz, 100 Hz, and 500 Hz,

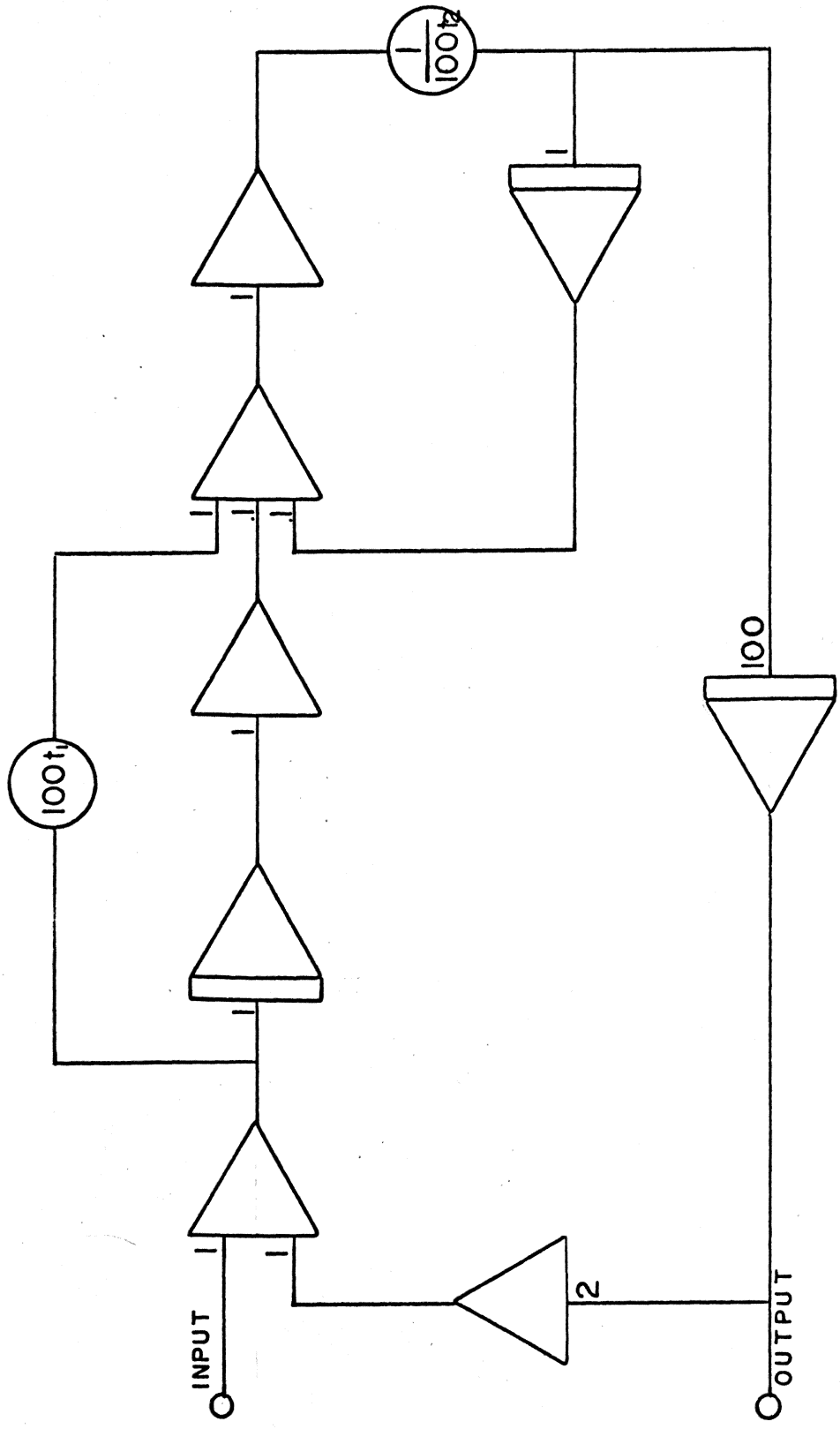

FIGURE 3.3-4 Scaled Simulation Program

respectively. The upper break frequency, t_1, was arbitrarily set at 1000 Hz.

Care should be taken to make sure that the Heath computer is perfectly balanced. The potentiometer which represents t_1 and determines the upper break frequency is indicated in Fig. 3.3-4 as 100 t_1. It is set to the desired value and then maintained constant throughout the experiment. The potentiometer indicated as 1/100 t_2 represents t_2 and determines the lower break frequency and the filter bandwidth. It is varied to provide the desired bandwidth. Figs. 3.3-5 through 3.3-9 are the loop responses obtained for the five different filter bandwidths subject to the same input of a step phase shift of 10 degrees. A digital computer program was available[16] for simulating analog computer operations. This was used to duplicate the results of Figs. 3.3-5 through 3.3-9 and the results are superimposed on Figs. 3.3-10 and 3.3-11 to show output phase and phase error, respectively, with filter bandwidth as a parameter. The computer program was also used to obtain the loop response to a frequency step (phase ramp). This result is shown in Fig. 3.3-12. In the digital computer simulation

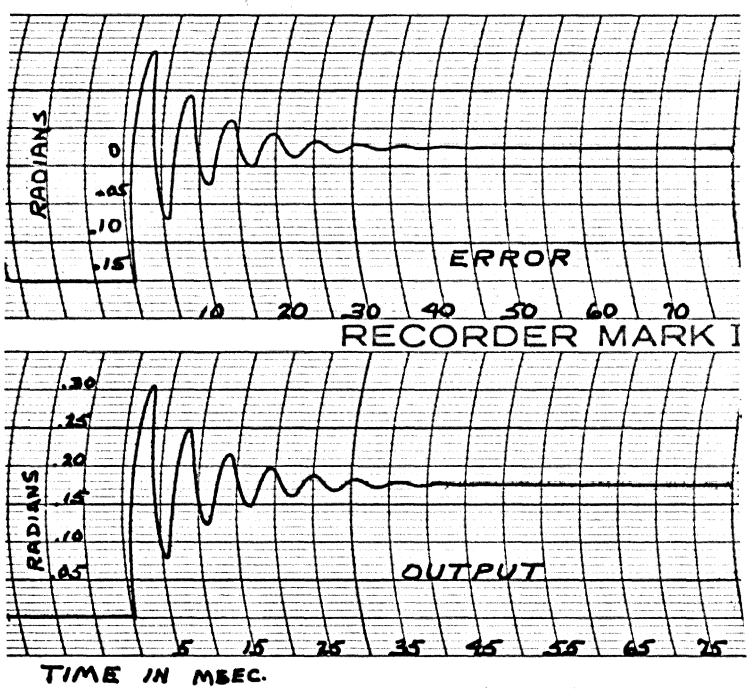

Phase Step of 10°

FIG. 3.3–5 PLL Response With 1 Hz. filter

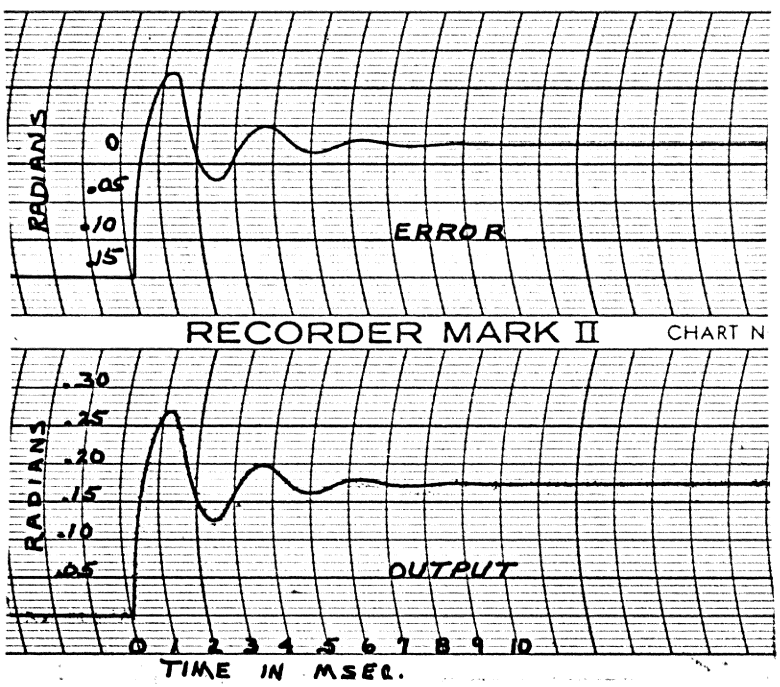

Phase Step of 10°

FIG. 3.3–6 PLL Response with 5 Hz. filter

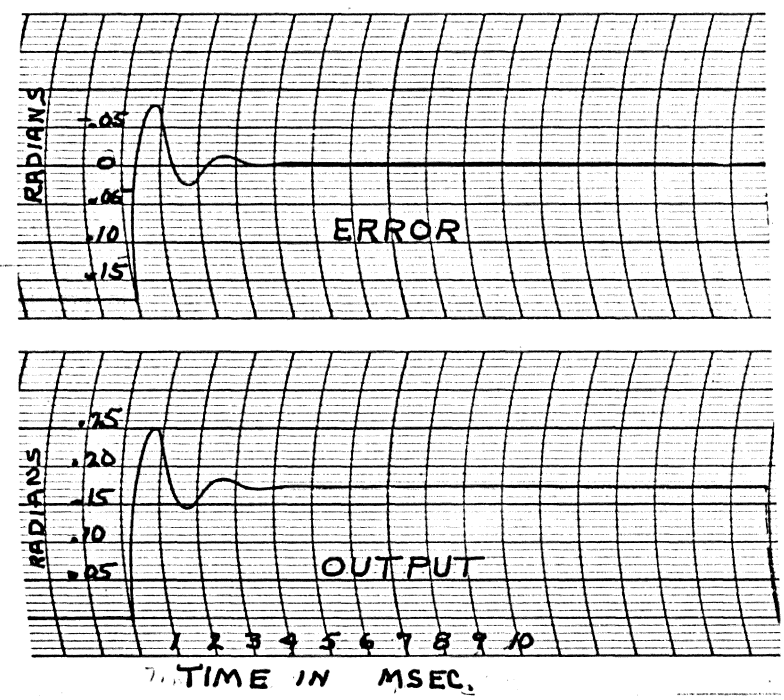

Phase Step of 10°

FIG. 3.3-7 PLL Response with 10 Hz filter

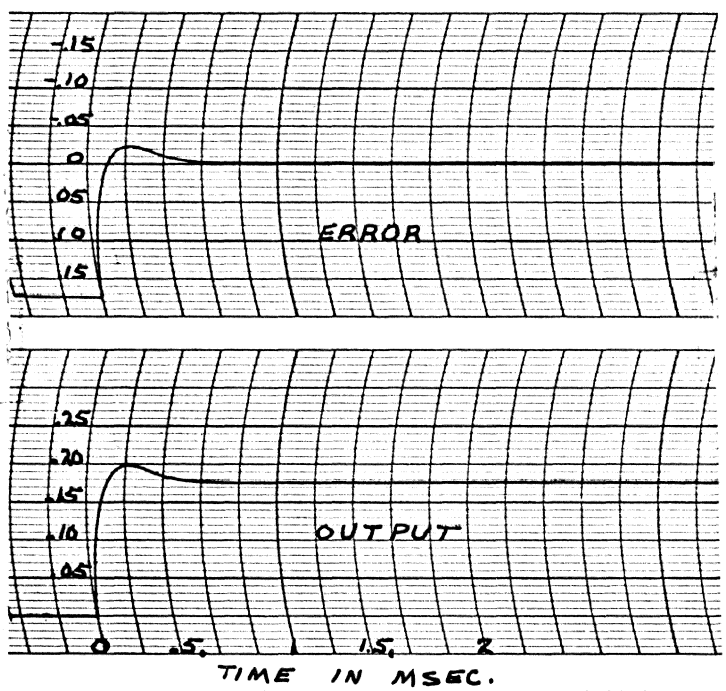

NOTE EXPANDED TIME SCALE
Phase Step of 10°

FIG. 3.3- 8 PLL Response with 100 Hz filter

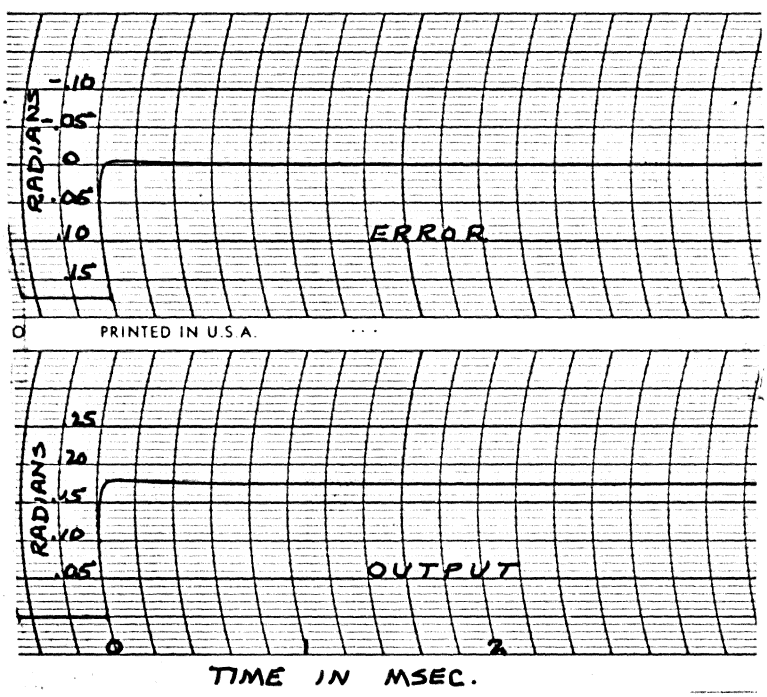

NOTE EXPANDED TIME SCALE

Phase Step of 10°

FIG. 3.3 – 9 PLL Response with 500 Hz filter

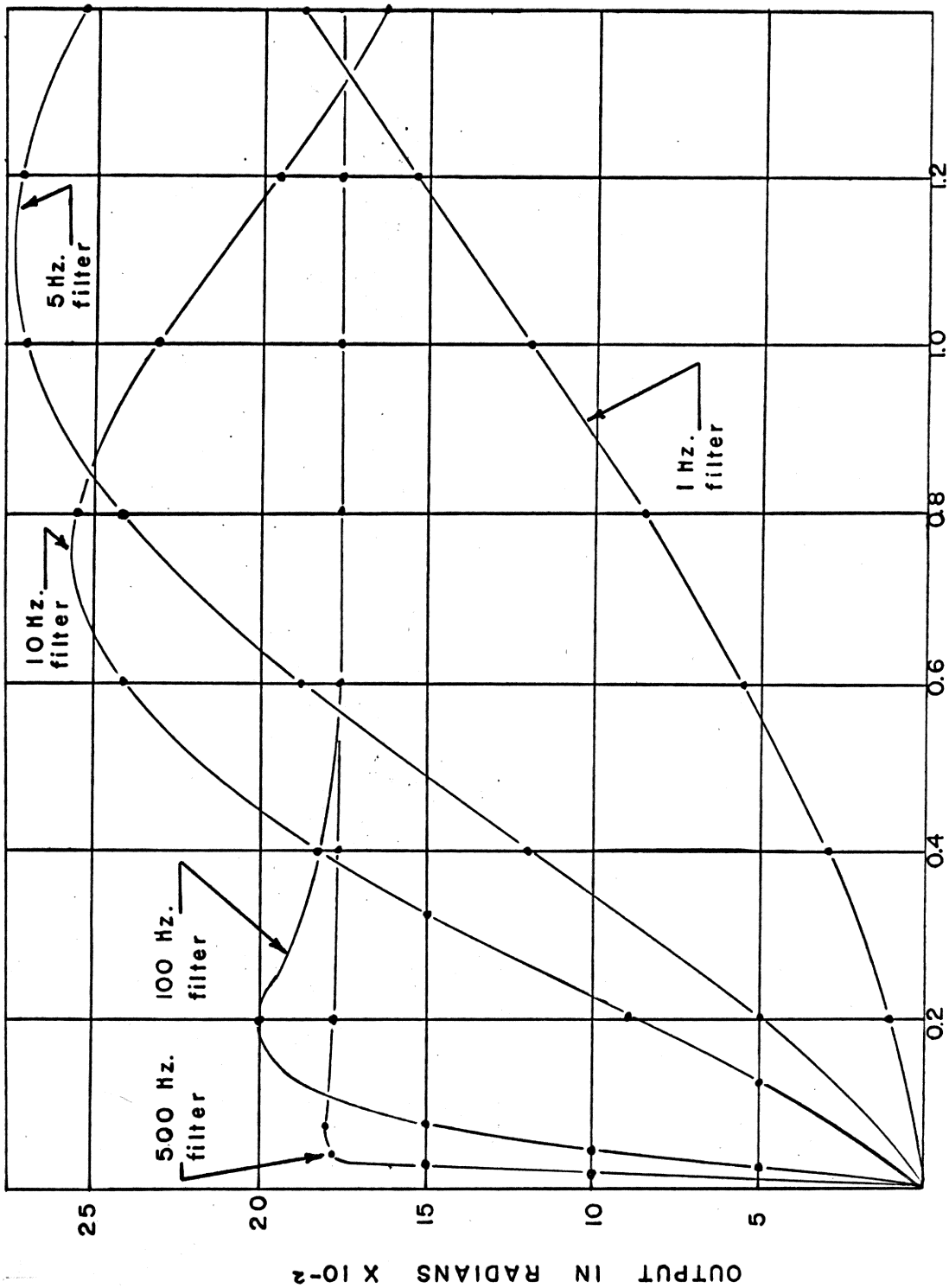

FIGURE 3.3-10 Response For 10 Degree Phase Step

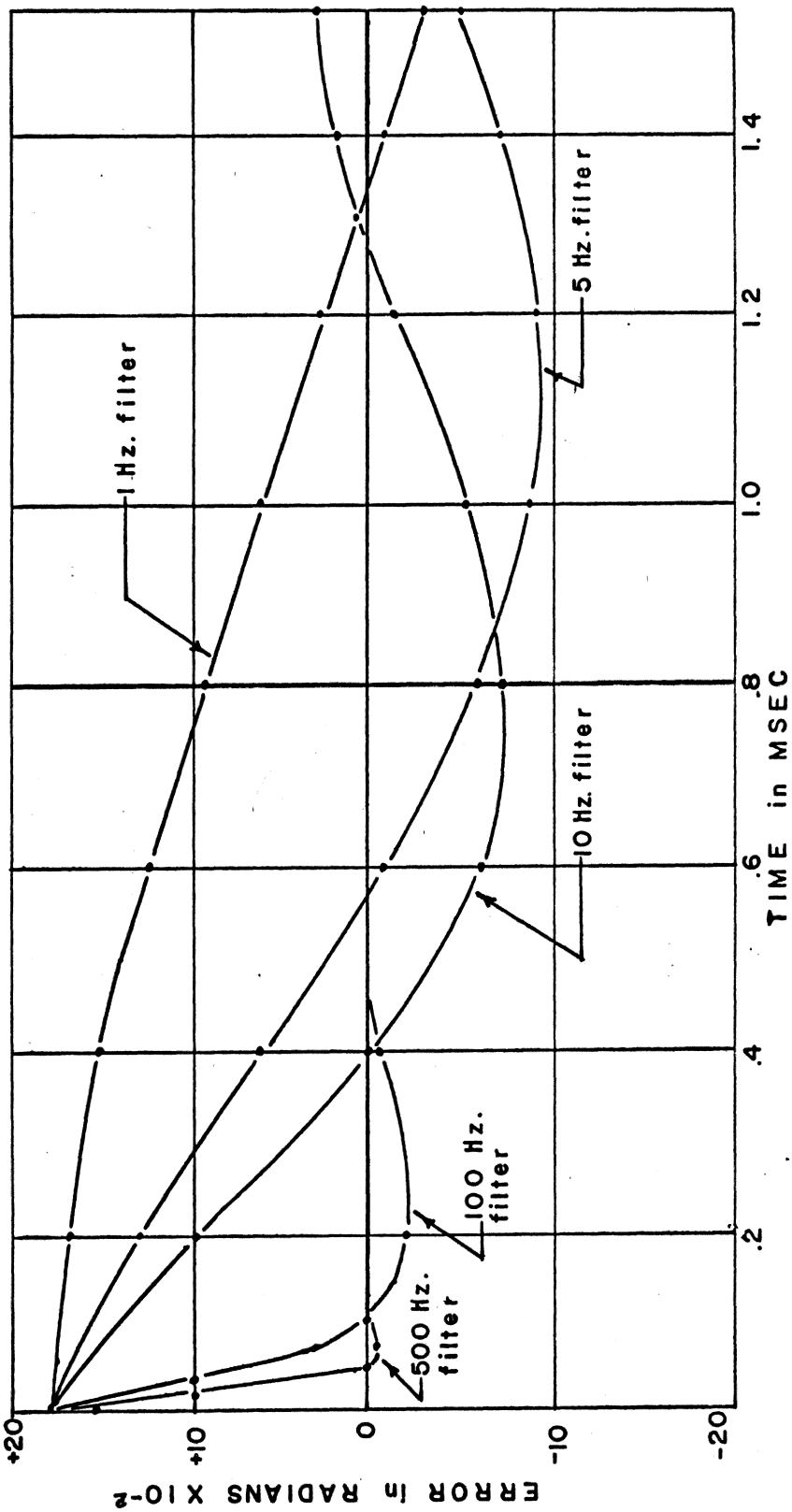

FIGURE 3.3-11 Error Response for Step Phase of 10°

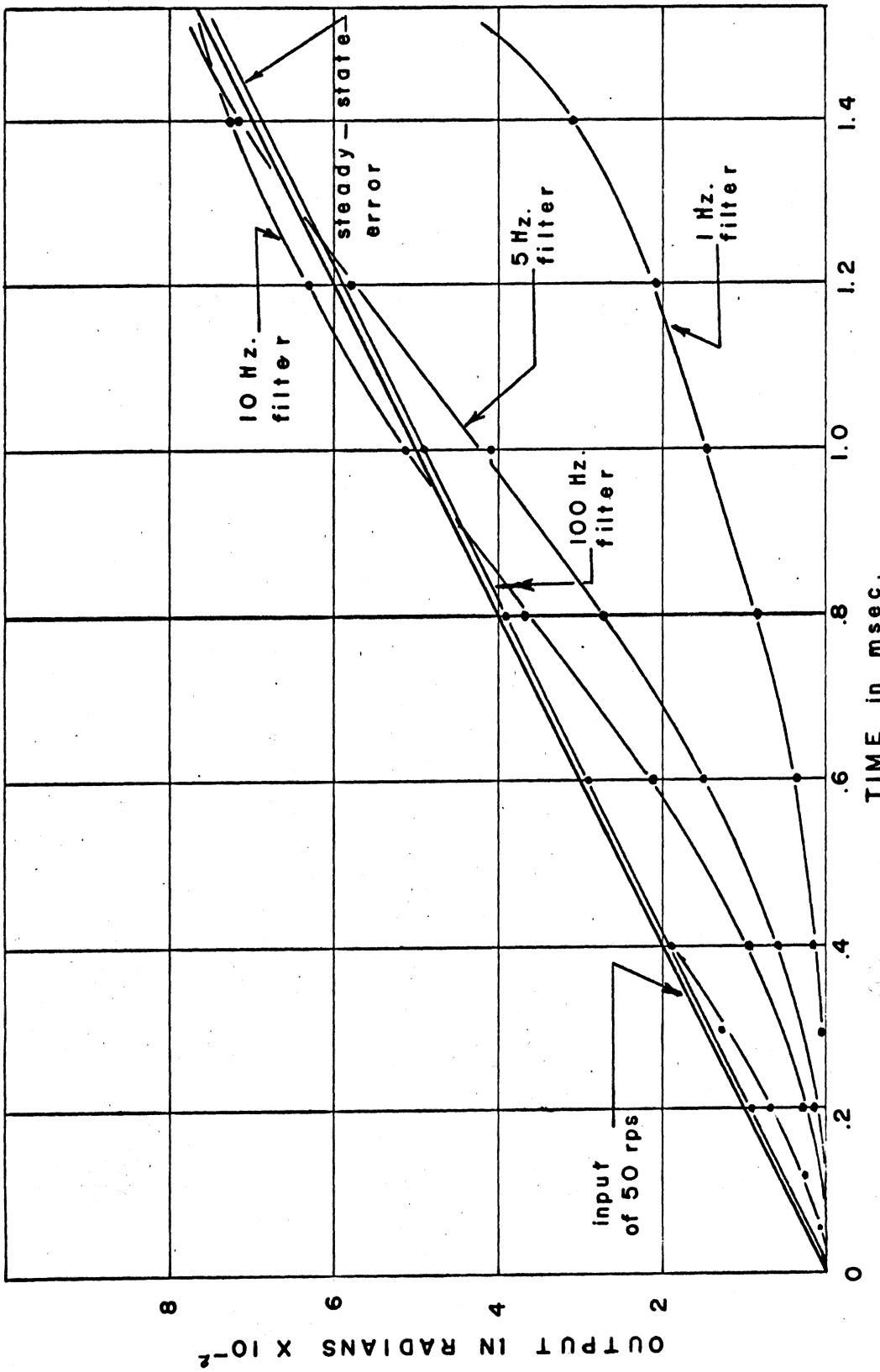

FIGURE 3.3-12 Response to Step of Frequency

the non-linear characteristic of the phase detector was taken into account.

The effect of the bandwidth of the low-pass filter on the time response of the loop can be clearly seen from the above results and thus the desirability of having a wide bandwidth.

IV. DESIGN OF ADAPTIVE FILTER

The results observed in the previous sections demonstrate the desirability of a filter which could have both a wide bandwidth and a narrow bandwidth. For this to occur simultaneously is clearly contradictory. A large bandwidth is needed when the system is out of lock to maximize the pull-in range and minimize the lock-in time. When the system is locked a narrow bandwidth filter is needed to minimize noise bandwidth. Thus if a system could be designed to have a changeable bandwidth we might achieve optimum performance under both conditions.

Bandwidth may be changed by several methods. A straightforward approach is to switch loop filter components. However, discreet changes in the system time constants can introduce transients which disturb the loop sufficiently to cause loss of lock. It is also feasible to switch the gain of the loop and change the over-all bandwidth, but the choice here will be to develop a continuously variable filter, which meets the desired requirements, and, at the same time avoid the discreet change transients. The basic filter which will be modified is the passive

filter shown in Fig. 2.1-1. The foremost prerequisite for an error sensing network is that it must have a very high input impedance. The error sensing network must not in any way effect the transfer function of the filter. A high input impedance field effect transistor amplifier will be used. The field effect transistor amplifier circuit is taken from Siliconix Incorporated application notes February, 1963, and is shown in Fig. 4.1-1 along with its a-c equivalent circuit. Calculations show that the input resistance is given by:

$$R_{in} = \frac{1}{(1 - A_v)(1/R_g + 1/r_{gs}) + 1/r_{gd}} \qquad (4.1\text{-}1)$$

where A_v is the voltage gain, R_g is as indicated on the figure, r_{gs} is the gate to source resistance, and r_{gd} is the gate to drain resistance, and is approximately 1250 megohms. The input capacitance is given by:

$$C_{in} = (1 - A_v)(C_{gs}) + C_{gd} \qquad (4.1\text{-}2)$$

where C_{gs} is the gate to source capacitance and C_{gd} is the gate to drain capacitance, and has a value of about 3.5 pf.

(a)

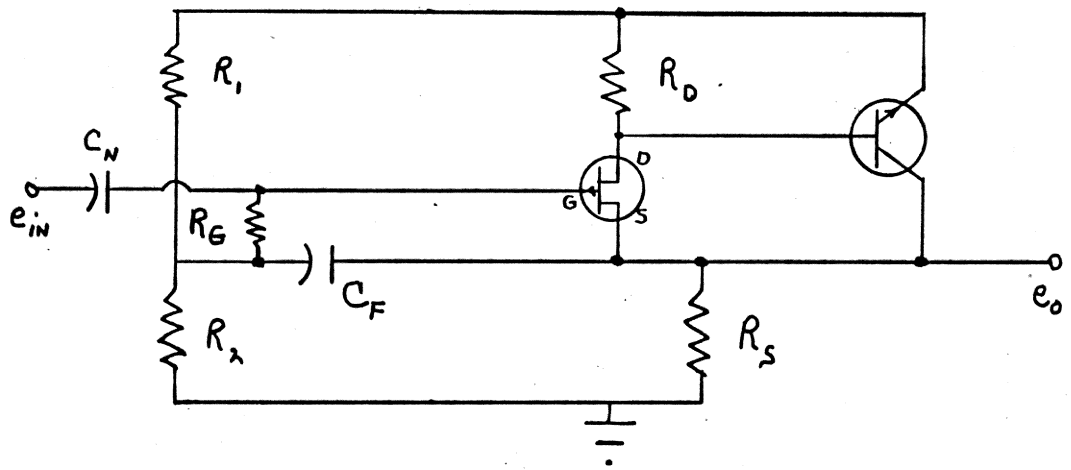

(b)

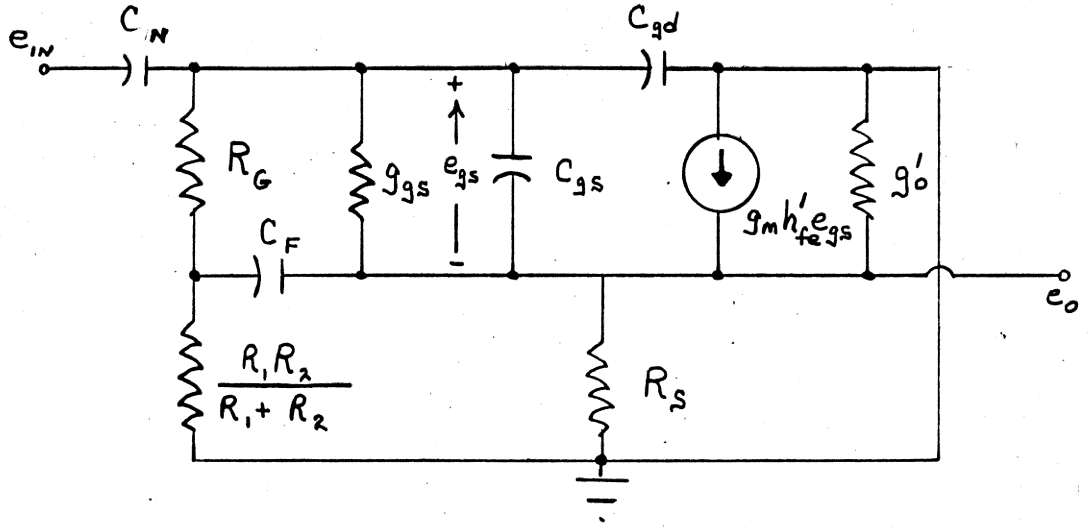

Fig. 4.1-1 (a) HIGH-INPUT Z AMPLIFIER
(b) EQUIVALENT CIRCUIT

The rest of the error sensing network can be a simple amplifier to get the desired voltage swing and a filter network which produces a d-c level to be used to bias the voltage-variable capacitors (varactors or varicaps). Varactors were used to obtain the variable bandwidth. The varactors are used in conjunction with an operational amplifier in a Miller[5] circuit. This was necessary due to the small values of varactors obtainable commercially and the large values needed for the filter to have a narrow bandwidth. The approximate input impedance of the Miller amplifier shown in Fig. 4.1-2 is:

$$Z_{in} = \frac{1}{1/R_1 + (1 + R_2/R_1)\ CS} \qquad (4.1\text{-}3)$$

where R_2/R_1 is the gain of the circuit, C is the feedback capacitor, R_1 is the input impedance. In the experimental filter the gain was arbitrarily chosen to be 100 and R_1 was set at 100 K to make the input impedance appear nearly a pure capacitance:

$$Z_{in} = \frac{1}{(R_2/R_1 + 1)\ CS} \qquad (4.1\text{-}4)$$

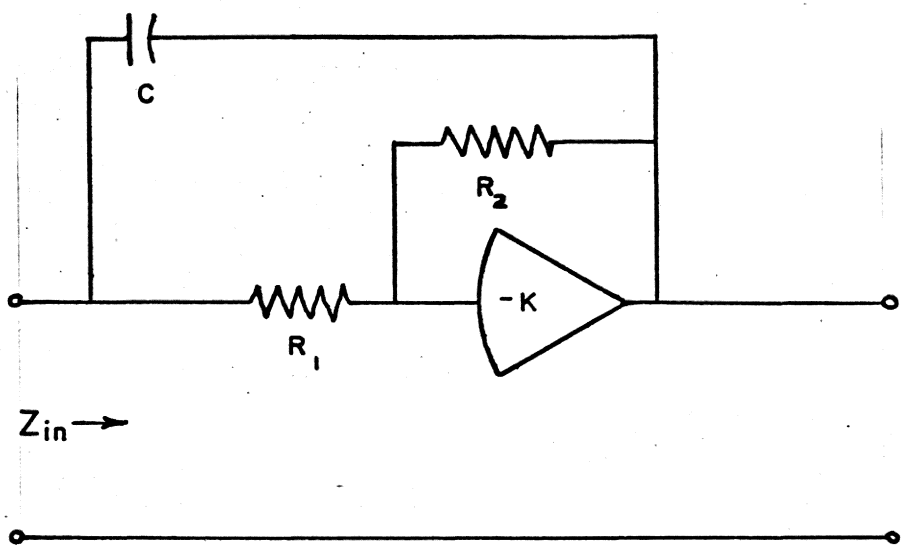

$$Z_{IN} = \frac{1}{1/R_1 + (1 + R_2/R_1)cs}$$

FIGURE 4.1-2 Miller Amplifier Circuit

Note here, that any change in C would also be multiplied by the gain of the circuit (R_2/R_1), allowing a much greater range of capacitance than would normally be possible with varactors alone. This capacitance multiplication would allow a designer to obtain a very large capacitance range by paralleling more of the varicaps. The complete circuit of the filter is shown in Fig. 4.1-3 and Table 4.1-1 is a complete parts list for the filter.

The varactors used were 1N953 which have a reverse break down voltage of 25 volts and a capacitance swing of 30-140 pf. The following equation which assumes an abrupt junction diode, is the equation relating the capacitance of the varactors to the applied voltage at the junction[8]:

$$C = C_m \sqrt{\frac{V_b + \phi}{v + \phi}} \qquad (4.1\text{-}5)$$

where V_b is the reverse voltage ratine, ϕ is the junction potential, C_m is the minimum capacitance, and v is the applied voltage bias.

Fig. 4.1-4 shows the approximate characteristic for the capacitors used in the filter. The junction potential was assumed to be 0.5 volt. The figure

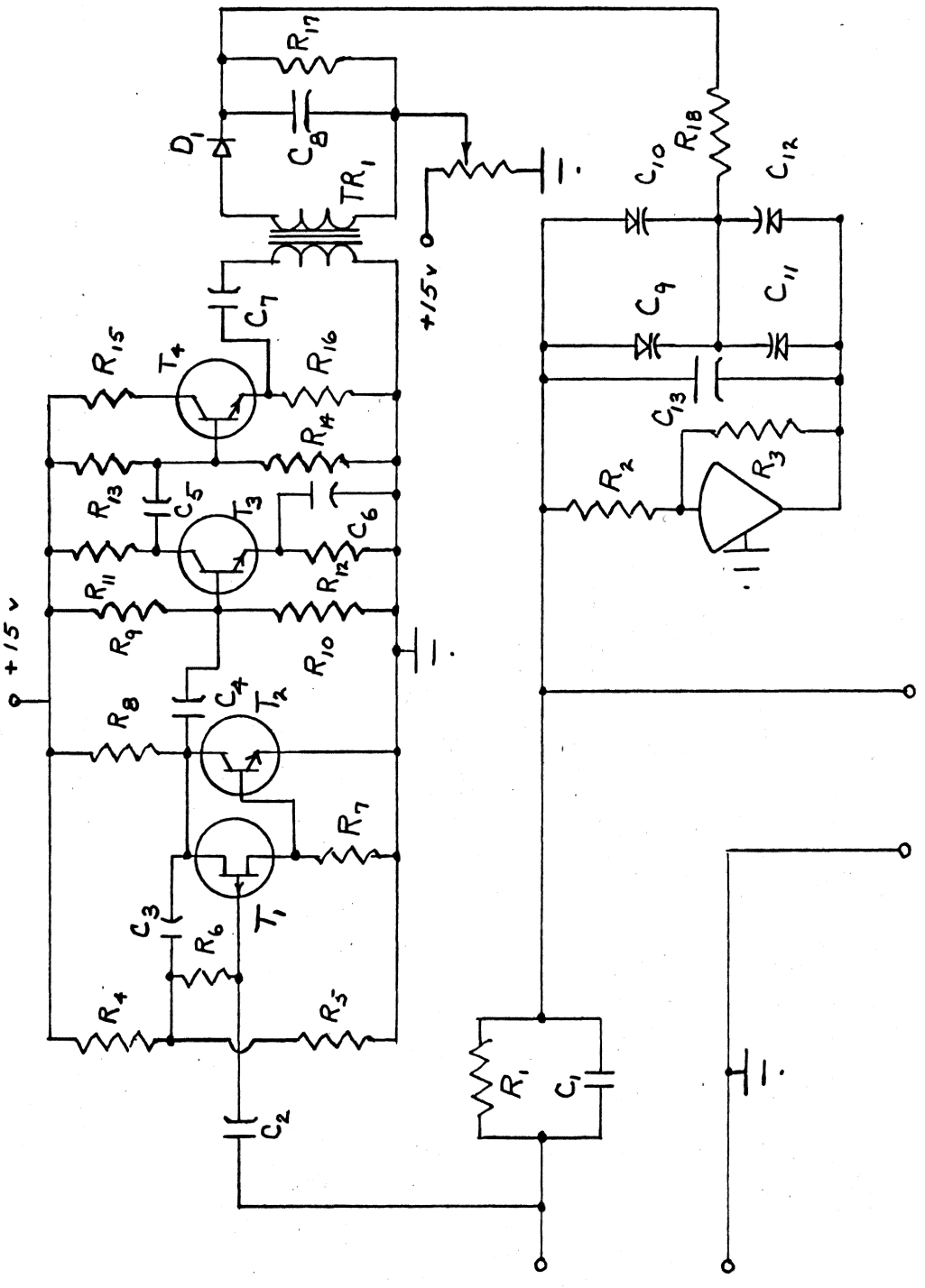

FIGURE 4.1-3 Dynamic Filter

Table 4.1-1

Parts List for Dynamic Filter

R_1 = 2 megohm
R_2 = 100K ohm
R_3 = 10 megohm
R_4 = 1.2 megohm
R_5 = 2.2 megohm
R_6 = 22 megohm
R_7 = 15K ohm
R_8 = 33K ohm
R_9 = 4700 ohm
R_{10} = 1000 ohm
R_{11} = 4700 ohm
R_{12} = 1000 ohm
R_{13} = 68K ohm
R_{14} = 68K ohm
R_{15} = 2200 ohm
R_{16} = 4700 ohm
R_{17} = 1 meg
R_{18} = 1 meg
C_1 = 100 pf
C_2 = 60 μf
C_3 = 10 μf
$C_{4,7}$ = 60 μf
C_8 = 25 μf
$C_{9,10,11,12}$ = 30-140 pf
C_{13} = 330 pf
T_1 = 2N2607
T_2 = 2N718
$T_{3,4}$ = 2N706
Trans. = 3 to 1 step up

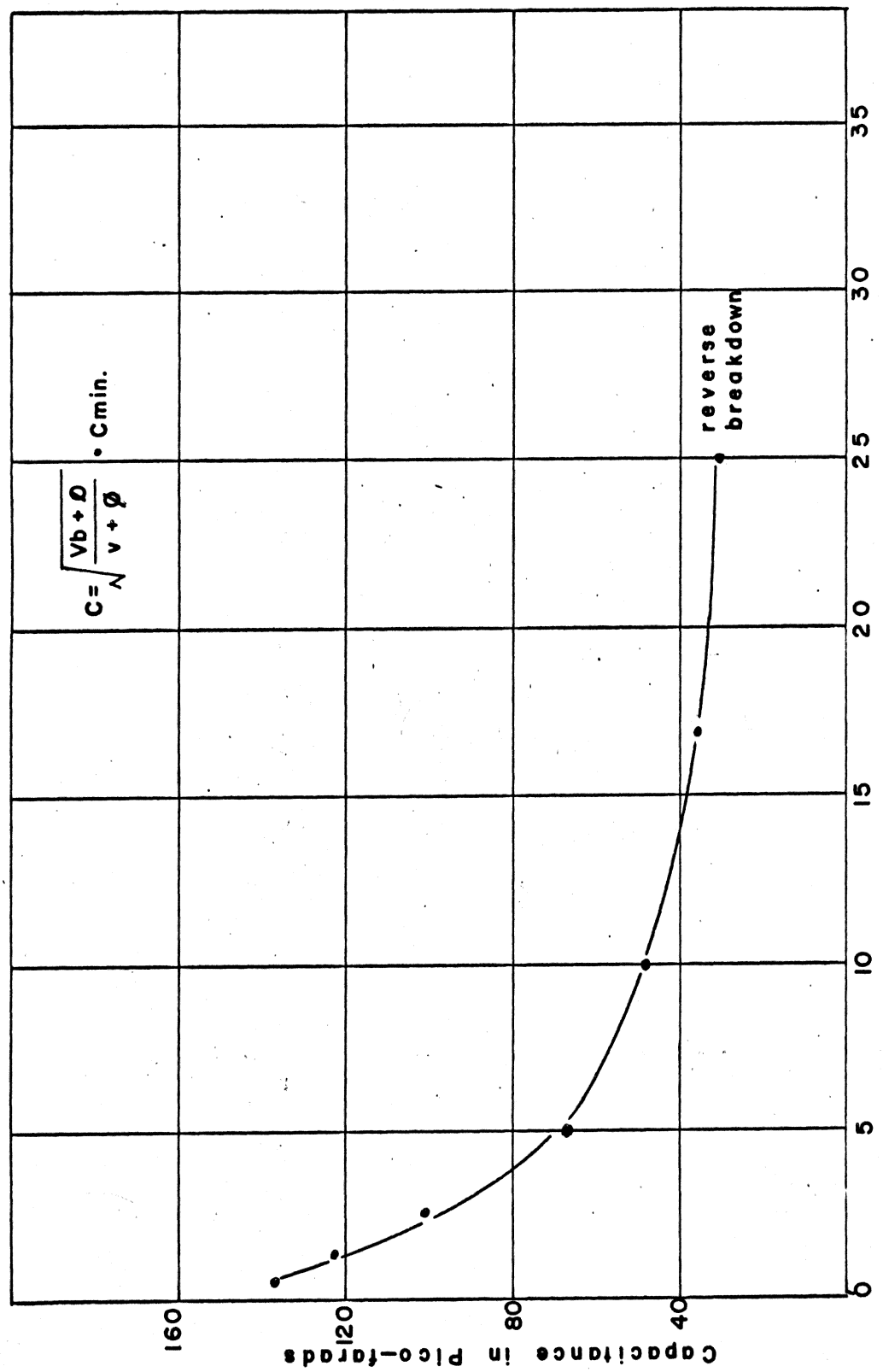

FIGURE 4.1-4 Capcitance Characteristic For IN953

clearly shows that the error network must supply approximately 20 volts from the error in order to obtain maximum range from the capacitors. Approximately one volt, peak-to-peak, at the input will provide the desired bias. The frequency response of the error sensing network is shown in Fig. 4.1-5, and it has a lower break frequence of approximately 25 hz.

Fig. 4.1-6 shows the frequency response of the filter with the bias on the varactors held constant at 1 volt and 23 volts, which represent approximately the maximum voltage swing possible for 1N953s. Thus the curve of Fig. 4.1-6 shows the change of filter bandwidth which may be achieved by varying the bias. With one volt, peak-to-peak, at the input of the loop, Fig. 4.1-7 demonstrates the effect of the low end response of the error network. Observe that as the frequency of the error signal increased, the slope of the response curve was decreased and at the higher frequencies the slope starts to approach that of the constant 23 volt bias condition. This tends to indicate that the dynamic capacitance is approaching the minimum of 30 pf and the total capacitance is approaching that of the constant capacitor alone.

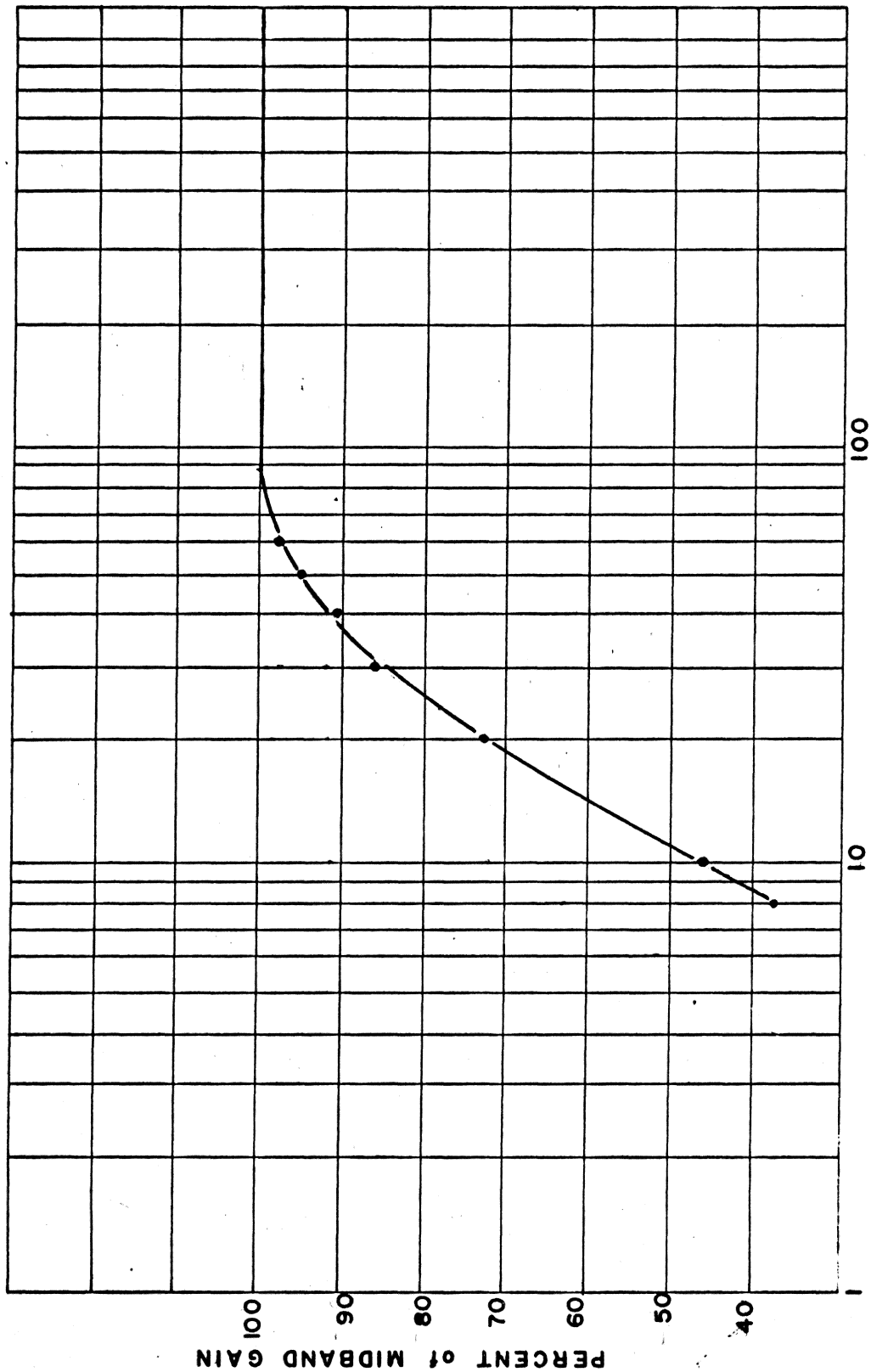

FIGURE 4.1-5 Frequency Response of Error Network

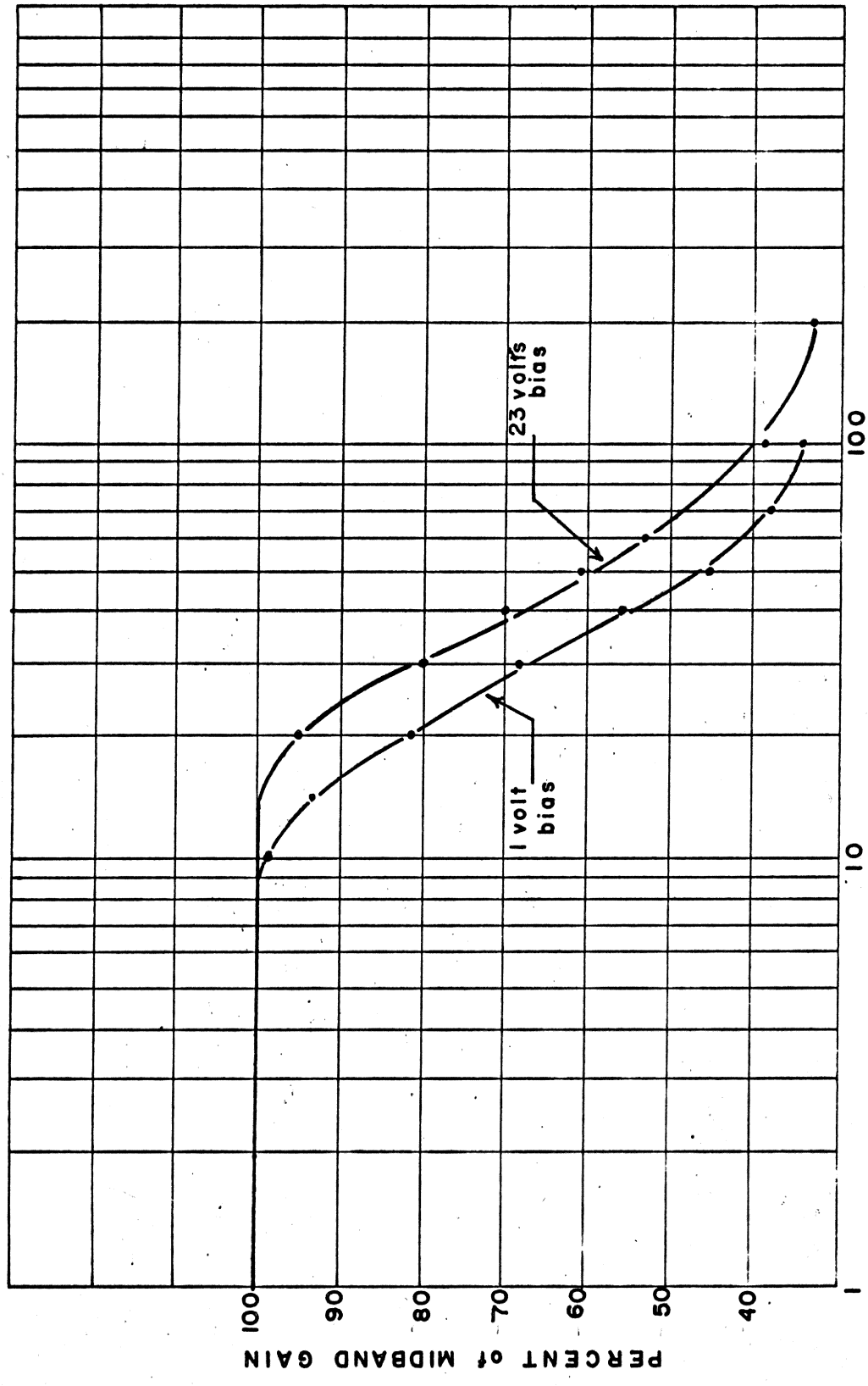

FIGURE 4.1-6 Frequency Response for Constant Bias

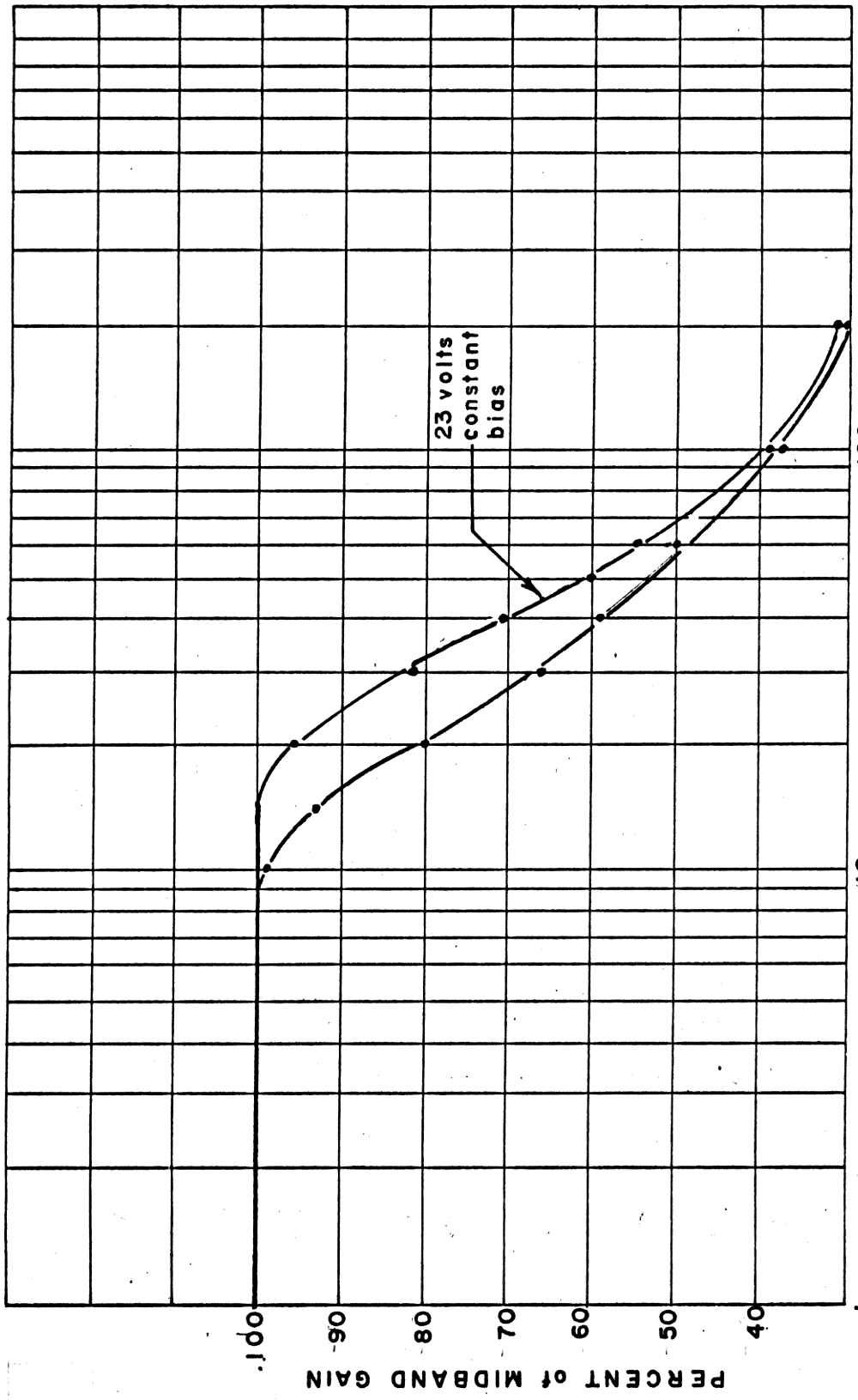

FIGURE 4.1-7 FILTER RESPONSE for 1 VOLT PEAK to PEAK INPUT

We can also note, by comparison of the frequency response of the error network with the frequency response of Fig. 4.1-7, that the slope appears to start its change somewhere around 20 to 37 cycles which is at the low end of the frequency response of the error network. This has the advantage of allowing a predetermined amount of error to be the point at which the low-pass filter will become active.

Table 4.1-2 is a list of test equipment used in this report.

Table 4.1-2

Test Equipment

1. Heathkit Electronic Analog Computer
   Number 4; Heath Company Subsidiary of Daystrom, Inc.
   Benton Harbor, Michigan

2. Brush Recorder Mark 11
   Brush Instruments
   Division of Clevite Corporation
   Number 1

3. Low Frequency Function Generator
   Model 202A, Number 1
   Hewlett Packard
   Palo Alto, California

4. Oscilloscope type 545
   Serial number 11951
   Tektronix, Inc.
   Portland, Oregon

5. Power Supply, Model 8650
   Range 0-40 volts, Number 5
   Harrison Laboratories

6. Voltmeter 427-A
   Hewlett Packard
   Range 0-30 volts, Number 5
   Palo Alto, California

V. DISCUSSION OF RESULTS

Rapid acquisition is possible by employing a filter with the ability to vary its bandwidth to fit the situation. For acquisition the loop should have a wide bandwidth, whereas for tracking the loop should have a narrowed bandwidth. From formulas presented and from the results of the analog simulation, it may be said that the pull-in range would be modestly increased, but the pull-in time would be drastically decreased. It is also apparent that increasing the bandwidth can only be done in cases of large signal-to-noise ratios because if increasing the bandwidth brings the system close to threshold, acquisition is not likely to occur.

Equations have shown the desirability of having the filter vary to fit the conditions. The noise bandwidth, noise power, and loop signal-to-noise ratio all are loop parameters which show marked improvement with the narrowing of the loop filter.

The dynamic filter designed to vary its bandwidth proved successful; however, the bandwidth swing was much smaller than desired. From Fig. 4.1-6 we observe that the bandwidth of the filter only varied by about 10 cycles and from Fig. 4.1-7 the lower cutoff

frequency of the error network also must be considered in the response of the loop.

Greater bandwidth swings could be obtained if more voltage variable capacitors were used and if the gain of the amplifier in the Miller circuit is increased. There are limitations here, of course; the voltage variable capacitors are quite expensive and the amplifier will easily saturate.

VI. SUMMARY AND CONCLUSIONS

Evidence has been presented which demonstrates the trade-off which is necessary in the design of phase-locked loops between the narrowness of the phase-locked loop bandpass, the speed with which the loop can respond, and the noise bandpass. Each of the above parameters has been tied directly to the bandpass of the filter. It has been shown that a wide bandpass filter is desirable if the designer wishes quick acquisition time and wide pull-in range, whereas, a narrow filter is desirable if he should require a minimum noise bandwidth. A filter which will provide for continuous changes in the bandwidth proportional to the error voltage which appears at the input to the filter was designed.

The effectiveness of the filter designed here left a lot to be desired because the bandwidth swing obtained was so limited; however, the feasibility of the approach was demonstrated. This is not necessarily the optimum method of providing an adoptive filter, but it appears to be one of the better approaches.

It can be concluded that it appears desirable to have a filter whose bandwidth that can be changed as desired

and the continuously changing filter appears to be the most desirable. The major disadvantage of the variable bandwidth filter is the deterioration of signal-to-noise ratios at the larger bandwidth. The effect of the filter on the dynamic loop is not known. The time required to change the bandwidth from a minimum to a maximum is determined by the propagation time through the isolation amplifier, the voltage amplifier, and the RC time constant of the smoothing filter on the output of the bias network. However, the majority of the lag will be made up of the RC time constant. Therefore, a natural extension of this work would be to build the complete system and test the network under dynamic conditions. This could not be simulated on the analog computer as the loop gain is such that the problem must be scaled and this includes the filter.

VIII. BIBLIOGRAPHY

Literature Cited

1. Gruen, W. J., "Theory of AFC Synchronization," Proc. IRE, Vol. 41, pp. 1043-1048, August 1953.

2. Jackson, Albert S., Analog Computation, McGraw-Hill Book Company, Inc., 1960, pp. 213-216.

3. Jaffe, R. M. and Rechtin, E., "Design and Performance of Phase-Locked Circuits Capable of Near-Optimum Performance over a Wide Range of Input Signal and Noise Levels," IRE Trans. on Information Theory, Vol. IT-1, pp. 66-76, March 1955.

4. Kuo, Benjamin C., Automatic Control Systems, Prentice-Hall, Inc., 1962, pp. 246-249.

5. Krauss, H. L., Skalnik, J. G., and Reich, J. H., Theory and Applications of Active Devices, p. 706, The Van Nostrand Series, 1966.

6. Lee, Y. W., Statistical Theory of Communication, John Wiley and Sons, Inc., 4th Printing, 1964, p. 162.

7. Lew, Wasyl M., "A Primer on Phase-Locked Loops," Electronic Design, July 20, 1964, pp. 56-60.

8. Penfield and Rafuse, Varactor Applications, The MIT Press, Massachusetts Institute of Technology, 1962, p. 66.

9. Richman, D., "Color-Carrier Reference Phase Synchronization Accuracy in NTSC Color Television," Proc. IRE, Vol. 42, pp. 106-133, January.

10. Scott, Norman R., Analog and Digital Computer Technology, McGraw-Hill Book Company, Inc., pp. 37-40, 1960.

11. Scott, Ronald E., Linear Circuits, Addison-Wesley Publishing Company, Inc., Copyright 1960.

12. Seshu, S. and Balabanian, Norman, Linear Network Analysis, John Wiley and Sons, Inc., Third Printing, November 1964.

13. Viterbi, A. J., "Acquisition and Tracking Behavior of Phase Locked Loops," JPL External Publication No. 673, July 14, 1959.

14. Viterbi, A. J., "Phase-Lock Loop System," Chapter 8, Space Communications, Editor, A. V. Balakrishman, McGraw-Hill Book Company, Inc., 1963.

15. Wright, R. R. and Skutt, R. H., Electronics Circuits and Devices, The Ronald Press Company, p. 185.

16. Street, Richard, Analog to Digital Simulation, Unpublished Thesis.

17. James, Nichols and Phillips, Theory of Servomechanisms, Vol. 25, Radiation Laboratory Series, McGraw-Hill Book Company, Inc., 1948.

Literature Reviewed

1. Anderson, R. C. and Merrill, F. G., "Crystal-Controller Primary Frequency Standards: Latest Advances for Long-Term Stability," Trans. IRE, 1-9, pp. 136-140, September 1960.

2. Attkinson, W. R. and Newman, J., "Spectrum Analysis of Extremely Low Frequency Variations of Quartz Oscillators," Proc. IRE, Vol. 51, p. 379, February 1963.

3. Benjaminson, A., "Phase-Locked Klystrons Simulate Doppler Radar," Electronics, pp. 44-46, April 19, 1963.

4. Benjaminson, A., "Phase-Locking Microwave Oscillators to Improve Stability and Frequency Modulation," Microwave Journal, pp. 88-92, January 1963.

5. Benjaminson, A., "Phase-Locked Microwave Oscillator Systems with 0.1 Cps. Stability," Microwave Journal, pp. 65-69, December 1964.

6. Boyle, P. J., "A Design Approach to Transistorized Voltage Controlled Oscillators," Electronic Design, pp. 22-27, March 1964.

7. Breese, M., Colbert, R., Rubin, W., and Sferrazza, P., "Phase-Locked Loops for Electronically Scanned Antenna Arrays," Trans. IRE, SET-7, pp. 95-100, December 1961.

8. Brockman, M. H., Buchanan, H. R., Choate, R. L., and Malling, L., "Extraterrestrial Radio Tracking and Communications," Proc. IRE, pp. 643-675, Vol. 48, April 1960.

9. Cahn, C. R., "Piecewise Linear Analysis of Phase-Lock Loops," Trans. IRE, SET-8, pp. 8-13, March 1962.

10. Charles, F. J. and Lindsey, W. C., "Some Analytical and Experimental Phase-Locked Loop Results for Low Signal to Noise Ratios," Proc. IEEE, Vol. 24, September 1966.

11. Choate, R. L., "Analysis of a Phase-Modulation Communication System," Trans. IRE, CS-8, pp. 221-227, December 1960.

12. Costas, J. P., "Synchronous Communications," Proc. IRE, Vol. 44, pp. 1713-1718, December 1956.

13. De Bey, L. G., "Tracking in Space by DOPLOC," Trans. IRE, MIL-4, pp. 332-335, April-July 1960.

14. Develet, Jr., J. A., "A Threshold Criterion for Phase-Lock Demodulator," Proc. IEEE, Vol. 51, pp. 349-356, February 1963.

15. Develet, Jr., J. A., "An Analytic Approximation of Phase-Lock Receiver Threshold," Trans. IEEE, SET-9, pp. 9-11, March 1963.

16. Enloe, L. H. and Rodda, J. L., "Laser Phase-Locked Loop," Proc. IEEE, Vol. 53, p. 165, February 1965.

17. Fitchen, F. C., Transistor Circuit Analysis and Design, D. Van Nostrand Company, Inc., May 1965.

18. Frazier, J. P. and Page, J., "Phase-Lock Loop Frequency Acquisition Study," Trans. IRE, SET-8, pp. 210-227, September 1962.

19. George, R. S., "Analysis of Synchronizing Systems for Dot-Interlaced Color Television," Proc. IRE, Vol. 38, pp. 124-131, February 1951.

20. Gilchriest, C. E., "Application of the Phase-Locked Loop to Telemetry as a Discriminator or Tracking Filter," Trans. IRE, TRC-4, pp. 20-35, June 1958.

21. Goldstein, A. J. and Byrne, C. J., "Pull-In Frequency of the Phase-Controlled Oscillator," Proc. IRE, Vol. 49, p. 1209, July 1961.

22. Gupta, S. C., "Transient Analysis of a Phase-Locked Loop Optimized for a Frequency Ramp Input," Trans. IEEE, SET-10, pp. 79-83, June 1964.

23. Gupta, S. C. and Sanneman, R. W., "Optimum Strategies for Minimum Time Frequency Transitions in Phase-Locked Loops," Trans. IEEE, Vol. AES-2, pp. 570-581, September 1966.

24. Laughlin, C. R., "The Diversity-Locked Loop--A Coherent Combiner," Trans. IEEE, SET-9, pp. 84-91, September 1963.

25. Leek, R., "Phase-Lock AFC Loops," Electronic and Radio Engineer, pp. 141-146, April 1957, and pp. 177-183, May 1957.

26. Malling, L. R., "Phase-Stable Oscillators for Space Communications, Including the Relationship Between the Phase Noise, the Spectrum, the Short-Term Stability, and the Q of the Oscillator," Proc. IRE, Vol. 50, pp. 1656-1665, July 1962.

27. Margolis, G. G., "The Response of a Phase-Locked Loop to a Sinusoid Plus Noise," Trans. IRE, IT-3, pp. 136-142, June 1957.

28. Martin, T. B., "Circuit Applications of the Field-Effect Transistor," Semicon. Prod., Vol. 5, Part 1, pp. 33-39, February 1962, Art. 11, pp. 30-38, March 1962.

29. McAleer, H. T., "A New Look at the Phase Locked Oscillator," Proc. IRE, Vol. 47, pp. 1137-1143, June 1959, Errata: 48, p. 1771, October 1960.

30. Mullen, J. A., "Background Noise in Oscillators," Proc. IRE, Vol. 48, pp. 1467-1473, August 1960.

31. Pedersen, B. O., "Phase-Sensitive Detection with Multiple Frequencies," Trans. IRE, 1-9, pp. 349-354, December 1960.

32. Peter, M. and Strandberg, W. P., "Phase Stabilization of Microwave Oscillators," Proc. IRE, Vol. 43, pp. 869-873, July 1955.

33. Pierce, John A., "Intercontinental Frequency Comparison by VLF Radio Transmission," Proc. IRE, Vol. 45, pp. 794-803, June 1957.

34. Preston, G. W., "Basic Theory of Locked Oscillators in Tracking FM Signals," Trans. IRE, SET-5, pp. 30-32, March 1959.

35. Preston, G. W. and J. C. Tellier, "The Lock-in Performance of an AFC Circuit," Proc. IRE, Vol. 41, pp. 249-251, February 1953.

36. Rey, T. J., "Automatic Phase Control: Theory and Design," Proc. IRE, Vol. 48, pp. 1760-1771, October 1960; Corrections in Proc. IRE, p. 590, March 1961.

37. Richman, D., "DC Quadricorrelator: A Two Mode Sync. System," Proc. IRE, Vol. 42, pp. 288-299, January 1954.

38. Rue, A. K. and Lus, P. A., "Transient Analysis of a Phase-Lock Loop Discriminator," Trans IRE, SET-7, pp. 105-111, December 1961.

39. Sann, K. H., "Phase Stability of Oscillator," Proc. IRE, Vol. 49, pp. 527-528, February 1961.

40. Sanneman, W. W. and Rowbotham, J. R., "Unlock Characteristics of the Optimum Type 11 Phase-Locked Loop," Trans. IEEE, ANE-11, pp. 15-24, March 1964.

41. Schlesinger, K., "Lock Oscillator for Television Synchronization," Electronics, Vol. 22, pp. 112-117, January 1949.

42. Smith, W. L., "Miniature Transistorized Crystal-Controller Precision Oscillator," Trans. IRE, 1-9, pp. 141-148, September 1960.

43. Strandberg, W. P., "Noise Spectrum of Phase-Locked Oscillators," Proc. IRE, Vol. 48, pp. 1168-1169, June 1960.

44. Van Valkenburg, M. E., Introduction to Modern Network Synthesis, John Wiley and Sons, Inc., 4th Printing, December 1965.

45. Van Trees, Harry L., "Functional Techniques for the Analysis of the Non-Linear Behavior of Phase-Locked Loops," Proc. IEEE, Vol. 52, pp. 894-911, August 1964.

46. Viterbi, A. J., "Phase-Locked Loop Dynamics in the Presence of Noise by Fokker-Planck Techniques," Proc. IEEE, Vol. 51, pp. 1737-1753, December 1963.

47. Wendt, K. R. and Fredendall, G. L., "Automatic Frequency and Phase Control of Synchronization of Television Receiver," Proc. IRE, Vol. 31, pp. 7-15, January 1943.

48. Holtzman, J. and A. K. Rue, "Regions of Asymptotic Stability for Loop," Trans. IEEE, SET-10, pp. 45-46, March 1964.

49. Weaver, C. S., "A New Approach to the Linear Design and Analysis of Phase-Locked Loops," Trans. IRE, SET-5, pp. 166-178, December 1959.

X. ACKNOWLEDGMENTS

The writer wishes to express his sincere appreciation to the many people who have helped him in any way towards completing this work. In particular, he is grateful to the following persons: to Dr. W. W. Cannon for the many suggestions pertaining to the technical aspects of the experimentation and also pertaining to the organization and actual writing of the thesis; to Professor Ralph R. Wright who assisted in the purchase of equipment needed to build the filter; to

for his assistance with the Digital Simulation Program; to for his assistance with the mechanics in the shop; to for her very efficient work in typing the manuscript; and to his wife and family who have been more than patient with him during this period.

The 4 page vita has been removed from the scanned document

The 4 page vita has been removed from the scanned document

The 4 page vita has been removed from the scanned document

The 4 page vita has been removed from the scanned document

APPENDIX A

Design Formulas

Loop Transfer Function:

$$\frac{\theta_o(s)}{\theta_i(s)} = \frac{K\ F(s)}{s + K\ F(s)} \qquad \text{(A-1)}$$

Second Order Loop:

$$H(s) = \frac{(2\zeta\omega_n - \frac{\omega_n^2}{K})\,s + \omega_n^2}{s^2 + 2\zeta\omega_n\,s + \omega_n^2} \qquad \text{(A-2)}$$

Noise Bandwidth:

$$B_L = \frac{K\tau}{t_2}\ \frac{K\ t_1^2 + t_2}{K\ t_1 + 1} \qquad \text{(A-3)}$$

Noise Threshold:

$$\begin{aligned} &\text{Unlock threshold:} && (SNR)_L = 1 \\ &\text{Acquisition threshold:} && (SNR)_L = 4 \end{aligned} \qquad \text{(A-4)}$$

Hold-in Range Static:

$$\Delta\omega_H = \pm\ K_v \text{ rad/sec.} \qquad \text{(A-5)}$$

Attention Patron:

Page 85 repeated in numbering

Hold-in Range Dynamic:

$$\Delta\omega_H = 1.8\,\omega_n\,(\zeta + 1) \text{ rad/sec.} \qquad \text{(A-6)}$$

Pull-in Range:

$$\Delta\omega_p = K\sqrt{2\,t_1/t_2} \qquad \text{(A-7)}$$

Pull-in Time:

$$\text{Frequency step:} \quad t_p = \frac{(\Delta\omega)^2\,t_2^{\,2}}{K\,(1 + K\,t_1)}$$

$$\text{Phase step:} \quad t_p = \frac{5\,t_2}{K\,t_1} \qquad \text{(A-8)}$$

Signal-to-Noise Ratio:

$$(SNR)_L = \frac{(SNR)_i\,B_i\,t_2}{K\,t_1} \qquad \text{(A-9)}$$

Steady-state Error:

$$\theta_v = \frac{\Delta\omega}{K_v} \qquad \text{(A-10)}$$

A PHASE-LOCKED LOOP STUDY, SIMULATION, AND DESIGN OF AN ADAPTIVE FILTER

by

Thomas Wayne Arthur

ABSTRACT

A thorough investigation of existing publications was conducted to determine the effect on phase-locked loop operation of the pass band of the low-pass filter in the loop. From the findings, it was concluded that when the loop was out of lock, the pass band of the low-pass filter should be wide; however, when the loop was locked, the pass band of the low-pass filter should be narrow.

The transient analysis of the loop demonstrated that it was desirable to have a wide pass band for the filter in order to minimize the lock-in time of the loop. An analog simulation of the loop verified the transient analysis. The loop simulation required the synthesis of the low-pass filter with operational building blocks in such a way that the pass band could be controlled as potentiometer settings.

The desirability of a variable pass band low-pass filter was established. The condition that the filter

must be able to sense when the loop was either locked or out of lock and adjust its pass band accordingly was set as a prerequisite for the design of a filter. A filter was built and tested which could meet the above conditions. The limited range of the filter left a lot to be desired; however, the feasibility of the approach was demonstrated.